การเปลี่ยนเถ้าลอยชานอ้อยเป็นสารประกอบโซเดียมซิลิเกต

นางสาวฐิติมาศ สุขสวัสดิ์ศักดิ์

จุฬาลงกรณ์มหาวิทยาลัย
Chulalongkorn University

วิทยานิพนธ์นี้เป็นส่วนหนึ่งของการศึกษาตามหลักสูตรปริญญาวิศวกรรมศาสตรมหาบัณฑิต
สาขาวิชาวิศวกรรมเคมี ภาควิชาวิศวกรรมเคมี
คณะวิศวกรรมศาสตร์ จุฬาลงกรณ์มหาวิทยาลัย
ปีการศึกษา 2556
ลิขสิทธิ์ของจุฬาลงกรณ์มหาวิทยาลัย

บทคัดย่อและแฟ้มข้อมูลฉบับเต็มของวิทยานิพนธ์ตั้งแต่ปีการศึกษา 2554 ที่ให้บริการในคลังปัญญาจุฬาฯ (CUIR)
เป็นแฟ้มข้อมูลของนิสิตเจ้าของวิทยานิพนธ์ ที่ส่งผ่านทางบัณฑิตวิทยาลัย
The abstract and full text of theses from the academic year 2011 in Chulalongkorn University Intellectual Repository (CUIR)
are the thesis authors' files submitted through the University Graduate School.

CONVERSION OF BAGASSE FLY ASH TO SODIUM SILICATE

Miss Titimat Suksawatsak

จุฬาลงกรณ์มหาวิทยาลัย
Chulalongkorn University

A Thesis Submitted in Partial Fulfillment of the Requirements
for the Degree of Master of Engineering Program in Chemical Engineering
Department of Chemical Engineering
Faculty of Engineering
Chulalongkorn University
Academic Year 2013

Copyright of Chulalongkorn University

Thesis Title	CONVERSION OF BAGASSE FLY ASH TO SODIUM SILICATE
By	Miss Titimat Suksawatsak
Field of Study	Chemical Engineering
Thesis Advisor	Associate Professor Prasert Pavasant, Ph.D.
Thesis Co-Advisor	Associate Professor Tawan Sooknoi, Ph.D.

Accepted by the Faculty of Engineering, Chulalongkorn University in Partial Fulfillment of the Requirements for the Master's Degree

.....Dean of the Faculty of Engineering

(Professor Bundhit Eua-arporn, Ph.D.)

THESIS COMMITTEE

.....Chairman

(Associate Professor Tharathon Mongkhonsi, Ph.D.)

.....Thesis Advisor

(Associate Professor Prasert Pavasant, Ph.D.)

.....Thesis Co-Advisor

(Associate Professor Tawan Sooknoi, Ph.D.)

.....Examiner

(Varun Taepaisitphongse, Ph.D.)

.....External Examiner

(Nawin Viriya-empikul, D.Eng.)

จุฬาลงกรณ์มหาวิทยาลัย
Chulalongkorn University

ฐิติมาศ สุขสวัสดิ์ศักดิ์ : การเปลี่ยนเถ้าลอยชานอ้อยเป็นสารประกอบโซเดียมซิลิเกต. (CONVERSION OF BAGASSE FLY ASH TO SODIUM SILICATE) อ.ที่ปรึกษาวิทยานิพนธ์หลัก: รศ. ดร. ประเสริฐ ภวสันต์, อ.ที่ปรึกษาวิทยานิพนธ์ร่วม: รศ. ดร. ตะวัน สุขน้อย, 68 หน้า.

งานวิจัยนี้ศึกษาการเปลี่ยนเถาลอยชานอ้อยเป็นสารประกอบโซเดียมซิลิเกตและมีการเปรียบเทียบร้อยละผลได้ของโซเดียมซิลิเกตจากเถ้าลอยชานอ้อยที่ไม่ผ่านการล้างกรดและเถ้าลอยชานอ้อยที่ผ่านการล้างกรด โดยการสังเคราะห์จะมีการใช้สารโซเดียมเพื่อกระตุ้นซิลิกาให้เกิดการสร้างเป็นสารประกอบโซเดียมซิลิเกต โดยโซเดียมที่ใช้ในการกระตุ้นสำหรับงานวิจัยนี้คือโซเดียมคาร์บอเนต จากการศึกษาองค์ประกอบออกไซด์ส่วนใหญ่ของเถ้าลอยชานอ้อยคือซิลิกาซึ่งจะมีอยู่ประมาณ 63%โดยน้ำหนัก และมีสารองค์ประกอบอื่นๆที่ปนเปื้อนเช่นอะลูมิเนียมออกไซด์ ,แคลเซียมออกไซด์,โพแทสเซียมออกไซด์ เป็นต้น ซึ่งมีอยู่ประมาณ 20%โดยน้ำหนัก สำหรับการปรับปรุงเถ้าลอยชานอ้อยเพื่อกัดสารปนเปื้อนก่อนการสังเคราะห์ใช้เทคนิคการล้างกรดด้วยกรดไฮโดรคลอริก พบว่าสารองค์ประกอบอื่นๆที่ปะปนในเถ้าลอยสามารถถูกกำจัดออกไปได้มากถึง 16%โดยน้ำหนัก โดยงานวิจัยนี้มีการศึกษาผลของสภาวะในการสังเคราะห์โซเดียมซิลิเกตต่อร้อยละผลได้ของโซเดียมซิลิเกตที่เกิดขึ้นทั้งเถ้าลอยชานอ้อยที่ไม่ผ่านการล้างกรดและเถ้าลอยชานอ้อยที่ผ่านการล้างกรดภายใต้สภาวะการสังเคราะห์ด้วยอัตราส่วนโมลของสารตั้งต้นซิลิกาต่อโซเดียมคาร์บอเนต (1:0.50-1:2.25), อุณหภูมิ (650-850°C) และระยะเวลาของการสังเคราะห์ 30-120 นาที จากผลการศึกษาพบว่าร้อยละผลได้ของโซเดียมซิลิเกตในปริมาณสูงสามารถสังเคราะห์ด้วยด้วยสภาวะที่เหมาะสมต่อการสังเคราะห์คืออัตราส่วนสารตั้งต้นซิลิกาต่อโซเดียมคาร์บอเนตคือ 1:1.25, อุณหภูมิของการสังเคราะห์คือ 830°C โดยใช้ระยะเวลาของการสังเคราะห์ 60 นาที ซึ่งผลของการสังเคราะห์พบว่าร้อยละผลได้ของสารละลายโซเดียมซิลิเกตและโซเดียมซิลิเกตที่ไม่สามารถละลายน้ำคือ 38%/18% และ 45%/18% สำหรับซิลิกาจากเถ้าลอยชานอ้อยและเถ้าลอยชานอ้อยที่ผ่านการล้างกรด

จุฬาลงกรณ์มหาวิทยาลัย
Chulalongkorn University

ภาควิชา วิศวกรรมเคมี ลายมือชื่อนิสิต .....

สาขาวิชา วิศวกรรมเคมี ลายมือชื่อ อ.ที่ปรึกษาวิทยานิพนธ์หลัก .....

ปีการศึกษา 2556 ลายมือชื่อ อ.ที่ปรึกษาวิทยานิพนธ์ร่วม .....

5570177821 : MAJOR CHEMICAL ENGINEERING
KEYWORDS: BAGASSE FLY ASH / ACID BAGASSE FLY ASH / SODIUM SILICATE / CONVERSION

TITIMAT SUKSAWATSAK: CONVERSION OF BAGASSE FLY ASH TO SODIUM SILICATE. ADVISOR: ASSOC. PROF. PRASERT PAVASANT, Ph.D., CO-ADVISOR: ASSOC. PROF. TAWAN SOOKNOI, Ph.D., 68 pp.

This work studied conversion of bagasse fly ash to sodium silicate synthesis and compared the yield of the total sodium silicate from bagasse fly ash (BFA) and acid washed bagasse fly ash (A-BFA). Sodium source employed here was sodium carbonate anhydrous (Na_2CO_3). Original bagasse fly ash contained mostly silica (63%wt) and other impurities, e.g. Al_2O_3, CaO, K_2O, etc. which could be up to 20%wt. Upon the acid washing with hydrochloric acid, most impurities (16%) was removed. The synthesis of sodium silicate was investigated under the range of operating conditions as follows: precursor mole ratio of SiO_2:Na_2CO_3 of (1:0.50-1:2.25), fused temperature (650-850°C) and reaction time (30-120 minutes). Yields of soluble/insoluble sodium silicate were 38%/18% and 45%/18% for BFA and A-BFA, respectively, which occurred at SiO_2:Na_2CO_3 mole ratio of 1:1.25, fused temperature 830°C and reaction time of 60 minutes.

จุฬาลงกรณ์มหาวิทยาลัย
Chulalongkorn University

Department:	Chemical Engineering	Student's Signature .....
Field of Study:	Chemical Engineering	Advisor's Signature .....
Academic Year:	2013	Co-Advisor's Signature .....

ACKNOWLEDGEMENTS

This thesis would not have been complete without the help and care of many people and coordinators whom are thankfully acknowledged here.

I would like to divide my genuine gratitude to my advisor Assoc. Prof. Dr. Prasert Pavasant for his valuable suggestions comments and inspiration all though my Master program. I also would like to thank my co-advisor Assoc. Prof. Dr. Tawan Sooknoi for his valuable idea and praise.

I would like to acknowledge local factory in Ratchaburi for providing the bagasse fly ash raw material and to extend special thanks to PTT Research and Technology Institute for financial support.

I would like to thank all friends and partners at Biochemical Engineering Laboratory (at Chulalongkorn University) for their friendship.

Most of all, I would like to thank my friends at Environmental and Safety Chemical Engineering Laboratory (at Chulalongkorn University) for their help and friendship. Special thanks are sincerely to Praewpakun Siltharm, Sudarat Phuklang, Eakkachai Khongkasem, Hathaichanok Rodrakhee, Patthama Sang, Panu Panitchakarn, Vatadta Ritcharoen, Puchong Sriouam for their in valuable suggestion.

จุฬาลงกรณ์มหาวิทยาลัย
Chulalongkorn University

CONTENTS

Page

THAI ABSTRACT iv
ENGLISH ABSTRACT v
ACKNOWLEDGEMENTS vi
CONTENTS vii
LIST OF TABLES x
LIST OF FIGURES xi
LIST OF EQUATIONS xiii
CHAPTER 1 INTRODUCTION 1
1.1 Motivations 1
1.2 Objectives 2
1.3 Scopes of this work 2
CHAPTER 2 BACKGROUNDS AND LITERATURE REVIEW 3
2.1 Bagasse fly ash 3
2.2 Utilization of fly ash 4
2.2.1 Composition of fly ash 4
2.2.2 Applications of fly ash 5
2.3 Sodium silicate 8
2.4 Sodium silicate from fly ash 11
CHAPTER 3 MATERIALS AND METHODS 13
3.1 Materials 13
3.2 Sodium silicate synthesis procedure 14
3.3 Acid washing process 14
3.4.1 Effect of SiO_2:Na_2CO_3 mole ratio 15
3.4.2 Effect of fused temperature 15
3.4.3 Effect of reaction time 15
3.5 Analysis of solid products 16
3.5.1 Sodium silicate in supernatant 16

จุฬาลงกรณ์มหาวิทยาลัย
CHULALONGKORN UNIVERSITY

Page

3.5.2 Solid precipitate 16
3.6 Analytical methods 17
3.6.1 Elemental Analyzer (CHNS/O) 17
3.6.2 X–Ray Fluorescence Spectrometer (XRF) 17
3.6.3 Thermogravimetric Analyzer (TGA) 17
3.6.4 X–Ray Diffractometer (XRD) 17
3.6.5 Inductively Coupled Plasma Optical Emission Spectrometer (ICP-OES) ... 17
CHAPTER 4 RESULTS AND DISCUSSION 18
4.1. Characterization of bagasse fly ash silica source 18
4.1.1 Composition of bagasse fly ash (BFA) and acid washed bagasse fly ash (A-BFA) 18
4.1.2 Thermal analysis 20
4.1.3 Structure analysis 21
4.2 Sodium silicate production 22
4.2.1 Effect of ratio of SiO_2:Na_2CO_3 on the formation of sodium silicate 22
4.2.2 Effect of fused temperature on sodium silicate production 29
4.2.3 Effect of reaction time on sodium silicate production 36
4.3 Polymerization of sodium silicate soluble 42
CHAPTER 5 CONCLUSIONS 44
5.1 Sodium silicate production 44
5.2 Contribution and Recommendations 45
REFERENCES 46
APPENDIX 50
VITA 68

จุฬาลงกรณ์มหาวิทยาลัย
Chulalongkorn University

LIST OF TABLES

Table 2.1 Classification systems of US standards ASTM C618 for fly ash..... 4
Table 2.2 Chemical composition of fly ashes from various sources 4
Table 2.3 Various applications of fly ashes..... 6
Table 2.4 Applications of sodium silicate..... 10
Table 2.5 Acid washing of fly ash to improved surface properties and removed impurity..... 11
Table 2.6 Sodium silicate Synthesis (Fusion)..... 13
Table 4.1 Elemental Components of BFA, A-BFA, and spent acid solution.....19
Table 5.1 Mass distribution in solid product at optimal condition of sodium silicate synthesis.....44

จุฬาลงกรณ์มหาวิทยาลัย
Chulalongkorn University

LIST OF FIGURES

Figure 2.1 Bagasse ash byproduct from sugar manufacture 3
Figure 2.2 Bridging oxygens and Non-bridging oxygens 8
Figure 3.1 Bagasse fly ash 13
Figure 3.2 Sodium carbonate anhydrous 13
Figure 3.3 Outline of experiments 14
Figure 4.1 TGA analysis of raw materials 20
Figure 4.2 XRD diffraction patterns of raw materials 21
Figure 4.3 Mass of products from BFA (a) and A-BFA (b) at various mole ratios of SiO_2:(x)Na_2CO_3 (830°C fused temperature, 60 minutes reaction time) 24
Figure 4.4 Mass distribution of various components in the fused products from BFA (a) and A-BFA (b) at various mole ratios of SiO_2:(x)Na_2CO_3 calculated base on total mass of raw materials for each condition (830°C fused temperature, 60 minutes reaction time) 26
Figure 4.5 XRD diffraction patterns of BFA (a) and A-BFA (b) products at various mole ratios of SiO_2:(x)Na_2CO_3 (830°C fused temperature, 60 minutes reaction time) 28
Figure 4.6 Mass of products from BFA (a) and A-BFA (b) at various fused temperatures (SiO_2:1.25Na_2CO_3 mole ratio, 60 minutes reaction time) 31
Figure 4.7 Mass distribution of various components in the fused products from BFA (a) and A-BFA (b) at various fused temperature calculated base on total mass of raw materials (SiO_2:1.25Na_2CO_3 mole ratio, 60 minutes of reaction time) 33
Figure 4.8 XRD diffraction patterns the solid products from BFA at various fused temperature (SiO_2:1.25Na_2CO_3 mole ratio, 60 minutes reaction time) 35
Figure 4.9 Mass of products from BFA (a) and A-BFA (b) at various reaction times (SiO_2:1.25Na_2CO_3 mole ratio, 830°C of fused temperature) 37
Figure 4.10 Mass distribution of various components in the fused products from BFA (a) and A-BFA (b) at various reaction time calculated base on total mass of raw materials (SiO_2:1.25Na_2CO_3 mole ratio, 830°C of fused temperature) 39
Figure 4.11 XRD diffraction patterns the solid products from BFA at various reaction times (SiO_2:1.25Na_2CO_3 mole ratio, 830°C of fused temperature 41
Figure 4.12 Polymerization of sodium silicate soluble 43

Figure 4.13 Polymerization pathway of pure silica 43

จุฬาลงกรณ์มหาวิทยาลัย
Chulalongkorn University

LIST OF EQUATIONS

Equation 2.1.....12
Equation 2.2.....12
Equation 4.1.....40
Equation 4.2.....40
Equation 4.3.....40
Equation 4.4.....42
Equation 4.5.....42

จุฬาลงกรณ์มหาวิทยาลัย
Chulalongkorn University

CHAPTER 1

INTRODUCTION

1.1 Motivations

Bagasse has been used increasingly as a raw material substitution for fossil fuel as it is renewable with relatively high heat capacity at about 18 MJ kg^{-1} (Jorapur & Rajvanshi, 1997). The burning of bagasse, although is considered carbon neutral, ends up with the generation of a large amount of fly ash that needs to be dealt with. Typically Bagasse Fly Ash (BFA) is landfilled which generates transportation and landfill costs. Local cost of landfill in Thailand was around 800-1,500 THB/ton depending on the locations of the plant and the landfill site. For a 10- ton coal fire boiler, about 10 tons of BFA is generated daily, and landfill of this BFA would cost 8,000-15,000THB/d.

However, analysis of bagasse indicates that it contains a large quantity of silica (SiO_2) which could be used in other applications. For instance, BFA can be applied to concrete construction for strength, corrosive resistance, for polymer reinforcement and heat resistance, and ceramics manufacturing. Sodium silicate from BFA poses one of the potential applications as this compound can be used as substrate for several processes such as catalyst synthesis, zeolites synthesis, wastewater treatment, construction and chemical compound etc.

BFA often contains quite a large quantity of metal contaminants such as iron(III) oxide (Fe_2O_3), aluminum oxide (Al_2O_3) etc. These metals can be removed by leaching with acid chloride because acid chloride reacts with metals and forms metal chloride salts and hydrogen gas. Metal chloride salts can then be washed by water, leaving a purer BFA as a solid precipitate.

Apart from the applications mentioned above, fly ash is also a potential source of silica which could be converted to several other compounds such as zeolites and silicate compounds. Both zeolite and sodium silicate are important feedstock used in several industries such as catalysts, detergents, ceramics, etc. Previous work in the Department of Chemical Engineering, Faculty of Engineering, Chulalongkorn University, proved that fly ash could be effectively converted to zeolites of various structures (Panitchakarn *et al.*, 2013).

This work, on the other hand, aimed to study the conversion of fly ash particularly bagasse fly ash (BFA) to sodium silicate. The investigation included the pretreatment of BFA with acid to enhance the purity of silica in BFA. The main objective was to examine the conditions that could best result in sodium silicate products.

1.2 Objectives

This work was set out to investigate the formation of sodium silicate from bagasse fly ash. The properties of sodium silicate as a function of synthesis condition were to be determined.

1.3 Scopes of this work

1.3.1 BFA was obtained from a local factory in Ratchaburi province in the year 2012. This was used as a silica precursor in this work.

1.3.2 Experiments were subjected to the following parameters:

- Manipulated variables
  - Molar ratio of SiO_2:Na_2CO_3 at 1:0.50-1:2.25
  - Reaction temperature at 650-850°C
  - Reaction time at 30–120 minutes
- Monitored parameters
  - Conversion of sodium silicate

จุฬาลงกรณ์มหาวิทยาลัย
Chulalongkorn University

CHAPTER 2

BACKGROUNDS AND LITERATURE REVIEW

2.1 Bagasse fly ash

Several small power plants use biomass as fuel. Due to the existing of noncombustible components, the burning of biomass generally ends up with both bottom and fly ashes. Generally, ash from combustion can be disposed of by landfill, but due to limited land area, landfill has not been a popular choice for wastes that can be converted to something else more useful.

Sugarcane is a main raw material for the sugar industry where the byproducts of the industry include bagasse, molasses and sludge. Bagasse is normally consumed as a source of fuel in the factory to substitute fossil fuels as it contains high content of carbon and hydrogen, which, despite a lower energy content than most fuels, can be used as bio-fuel. Due to the high ash content of more than 25%wt (Kim *et al.*, 2013), ash is left from the burning of bagasse. In other words, the combustion of one ton of bagasse generates approximately 250 kg of fly ash. This ash is mixed with the hot gas and blown out of the smokestacks of the burner (see Figure 2.1).

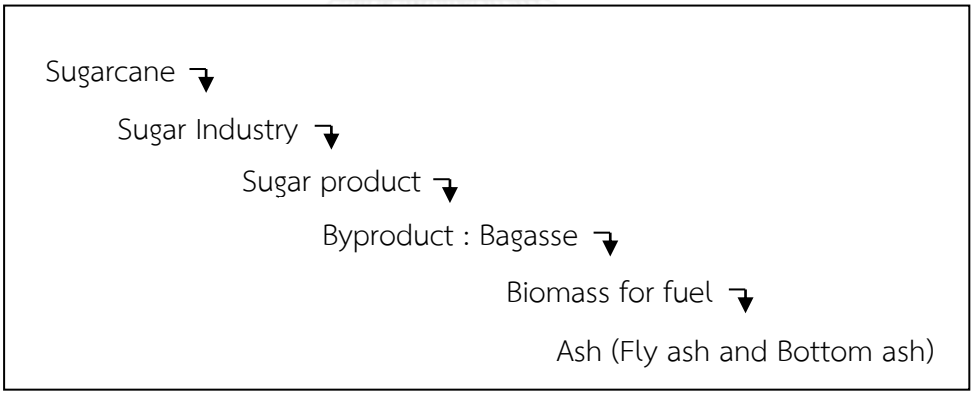

Figure 2.1 Bagasse ash byproduct from sugar manufacture

2.2 Utilization of fly ash

2.2.1 Composition of fly ash

Fly ash is comprised of several components which are mostly oxides of both metals such as aluminum, iron, magnesium, calcium and non-metals, such as sulfur but the major element is silicon dioxide (Ruangtaweep *et al.*, 2011). Fly ash can be classified by The American Society for Testing and Materials (ASTMs) as in Table 2.1 (Blissett & Rowson, 2012). The other types of biomass were examined for their chemical compositions by XRF analysis as summarized in Table 2.2.

Table 2.1 Classification systems of US standards ASTM C618 for fly ash

Class	% Weight			
	SiO_2+Al_2O_3+Fe_2O_3 (%)	SO_3 (%)	Moisture (%)	*LOI (%)
C	>50	<5	<3	<6
F	>70	-	-	<12

* %LOI=%Loss on Ignition

Table 2.2 Chemical composition of fly ashes from various sources (Umamaheswaran & Batra, 2008)

Kind / Composition	% Weight			
	Sub-bituminous fly ash	Lignite fly ash	Rice husk fly ash	Bagasse fly ash
SiO_2	40-60	15-45	93.52	65.03
Al_2O_3	20-30	10-25	0.01	0.49
Fe_2O_3	4-10	4-15	0.51	0.49
TiO_2	-	-	0.04	0.08
P_2O_5	-	-	1.06	1.14
CaO	5-30	15-40	0.68	2.75
MgO	1-6	3-10	0.47	3.26

2.2.2 Applications of fly ash

Fly ash is waste from combustion but it contains a large quantity of silica and therefore many studies have investigated potential conversion applications of such fly ash to useful products. The different compositions enable the use of fly ash in various applications such as construction, additives in polymeric materials, adsorbents, anti-rust, ion-exchanger, formation of catalyst/mesoporous material, and another chemical compounds as illustrated in Table 2.3 below.

จุฬาลงกรณ์มหาวิทยาลัย
Chulalongkorn University

Table 2.3 Various applications of fly ashes

Application/ Product	Direction	Conditions, Reaction and Reason	Properties	References
Construction	Cement component	- Mix with cement up to 50%wt	- Better strength - Better durability	(Yang *et al.*, 2008)
		- Mix with Portland cement up to 90%wt - Fly ash, Portland cement and rubber waste mix with weigh ratio 2:1:7	- Improving mechanical properties for construction - Increasing strength - Reducing water for mixture	(Yilmaz & Degirmenci, 2009)
	Geopolymer material	- Activation by alkali catalyst - Low cost	- Good mechanical properties - Fire resistance - Low density - Better chemical resistance	(Blissett & Rowson, 2012)
	Fly ash bricks	- Production at room temperature - Reducing energy costs	- Replacing clay - Better durability and strength	(Chindaprasirt & Pimraksa, 2008)
		- Mix with other composition - Fly ash pretreatment required	- Resistance to heat - Replacing brick construction	(Fernández-Pereira *et al.*, 2011) and (Cultrone & Sebastián, 2009)

Table 2.3 Various applications of fly ashes (Cont.)

Application/ Product	Direction	Conditions, Reaction and Reason	Properties	References
Polymer	Polymer binder	- Additive for polymer - Use for concrete-link polymer composite	- Replacing more than 50%wt - Increasing mechanical and chemical properties	(Garbacz & Sokołowska, 2013)
Catalyst/ Mesoporous material	Adsorbents	- Mix with calcium oxide and spread out in soil	- Improving stability in soil - Exchanging metal ions by electric force	(Blissett & Rowson, 2012)
	Precursor for synthesis	- Hydrothermal reaction - Temperature 80°C - Reaction time 6 hours	- Synthesis of zeolite A - Good distribution of zeolite by ultrasonic system	(Musyoka *et al.*, 2012)
		- Hydrothermal reaction - Reaction time 12 hours	- Synthesis of zeolite X - Reducing temperature during hydrothermal step by sonication pre-treatment technique	(Belviso *et al.*, 2011)
		- Hydrothermal reaction - Temperature 100°C - Reaction time 120 hours	- Synthesis of zeolite MCM-41material - Surface area reduced by 33%.	(Misran *et al.*, 2007)

2.3 Sodium silicate

Sodium silicate is common name for combinations with the prescription of $Na_2(SiO_2)_nO$. Silica (SiO_2) can be applied as raw material for some chemical compounds such as sodium silicate (Na_2SiO_3). Sodium silicate is composed of sodium and silicate in the molecular structure and is used in several industrial applications (Yang et al., 2008). The demand of sodium silicate increases continually and the amount was anticipated to increase at the rate of 0.4% per year in Thailand for the replacement of silica materials in Portland cement industry (Davidovits, 2008).

Sodium silicate is the combination of silicon and oxygen in various structures. The sodium (alkali) source activated some the bridging oxygen (BOs) into non-bridging oxygen (NBOs), effectively decreasing the polymerization of the silica network structure. So, sodium ions form new bonds with NBOs to sodium silicate (Zhao et al., 2012). This structure is shown in Figure 2.2.

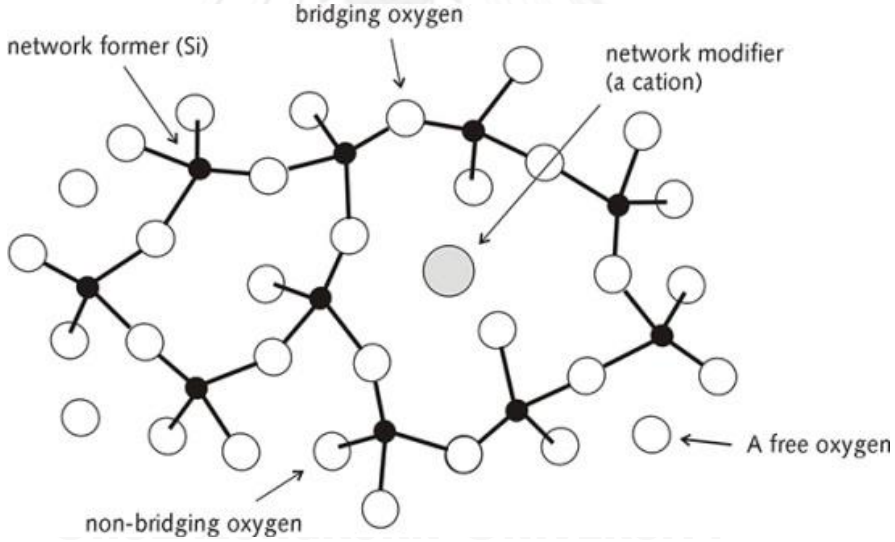

Figure 2.2 Bridging oxygens and Non-bridging oxygens

Soluble sodium silicate is widely used in chemical industries, e.g. as buffer solution, improvement of surface materials, improvement surface and thermal properties and polymer viscosity, precursor of zeolites and other petrochemical compounds. Besides, it can also be used in cleaner, washing or detergent products, ceramics, construction and soil improving additive. Table 2.4 is a brief summary of the usability of sodium silicate.

Soluble sodium silicate had composition by a molar ratio SiO_2:Na_2O of 1.8-4.0 (Böschel *et al.*, 2003), polysilicate ions or colloids have a condensation polymerization internal structure and surface covered by silanol groups. Chemical equilibrium between monomeric and polymeric anions in aqueous sodium silicate solution occurs with SiO_2:Na_2O molar ratios of 1.0 to 0.5. Concentrated sodium silicate solution could be kept for long time, whereas diluted solutions are influenced by aging time. The strongest parameter controlling the stability and structure of sodium silicate is pH.

จุฬาลงกรณ์มหาวิทยาลัย
Chulalongkorn University

Table 2.4 Applications of sodium silicate

Usability	Features and Benefits	References
Bone like Coating	- Activate nucleating layer of materials - Increase tissue surface - Improve hydrophobic property	(Oliveira *et al.*, 2003)
Glass	- Change physical characteristics from hydrophobic to hydrophilic	(Yamashita et al., 2008)
Modified surface	- Increase adsorption mechanism	(Yang et al., 2008)
	- Anti-rust - Improve hydrophobic property	(Gaggiano *et al.*, 2011)
	- Anti-rust - Smooth surface material	(Yuan *et al.*, 2011)
Binder for cement	- Improve mechanical properties	(Ravikumar & Neithalath, 2012)
Zeolites synthesis	- Increase crystal of zeolite	(Karami & Rohani, 2009)
	- Good morphology	(Round *et al.*, 1997)
	- Increase crystal of zeolite	(Bo & Hongzhu, 1998)
	- Complete crystal of zeolite for polymer membrane - Low thickness membrane - Enhance separation performance	(Ge *et al.*, 2012)
	- Increase performance of catalyst	(Chareonpanich *et al.*, 2004)
Solid base catalyst	- Replace solid base catalyst - Lose of base catalyst - Reduce reaction time - Increase yield of biodiesel - Recycle base catalyst	(Guo *et al.*, 2010)
		(Long *et al.*, 2011)

จุฬาลงกรณ์มหาวิทยาลัย
Chulalongkorn University

2.4 Sodium silicate from fly ash

Sodium silicate is commonly manufactured by the alkali method where alkali activates and converts fly ash to sodium silicate (Ravikumar & Neithalath, 2012). The completion of the reaction depends on several factors, such as reaction time, proportion of silica source to alkali source. Silica source is also a major concern for this production as it will affect the cost of manufacture quite considerably (Garbacz & Sokołowska, 2013). Examples of silica sources are silica sand, silica quartz, silica amorphous, glass, fly ash, etc. In both economic and environmental points of view, fly ash is one of the preferred raw materials as it is generally present in large quantity and otherwise it will need to be disposed of (Kashiwakura *et al.*, 2010). However, fly ash also carries with it a large number of impurities which requires either pre- or post-purification (Kow *et al.*, 2014).

Typically impurities in fly ash can be removed by acid washing where acid reacts with metal oxide to form soluble metal compounds which can be washed with water and removed from the ash. Table 2.5 summarizes literature details on the effect of acid washing on the purity and particle properties of fly ash silica source where common acids used for this purpose include hydrochloric and sulfuric acids which were reported to be effective in removing trace metal impurities. The acids also improve the solid surface of fly ash as a better particle distribution of silica source could be resulted from acid treatment.

Table 2.5 Acid washing of fly ash to improved surface properties and removed impurity

Condition for acid washing		Effect		References
		Solid surface	Removed metal	
Ammonium nitrate	3 mol/L	-	Copper	(Karlfeldt Fedje *et al.*, 2010)
Hydrochloric acid		Clean solid surface	Aluminium	
	1 mol/L	-	Boron	(Kashiwakura *et al.*, 2009)
Sulfuric acid		Better particle distribution	Aluminium	(Iyer, 2002)
		-	Arsenic	(Kashiwakura et al., 2010)

Sometimes, carbon source still remains in the fly ash (not complete combustion of bagasse), oxygen must also be added to the reactor to remove the remaining carbon as stated in Equation 2.1.

$$C(s) + SiO_2(s) + O_2(g) \longrightarrow SiO_2(s) + 2CO_2(g) \qquad \text{Equation 2.1}$$

To produce sodium silicate, several alkali sources can be selected such as lithium, sodium and potassium. These alkali are mixed with silica source and activate silica to alkaline silicate. Various alkali sources offer different reaction kinetics (Ravikumar & Neithalath, 2012). Among the various alkali, sodium is perhaps the most common. There are many sodium compounds that can be used as an activating agent, e.g. sodium hydroxide, sodium sulfate, sodium carbonate and sodium phosphate. Sodium hydroxide often creates a mixing problem as it tends to pile up in the reactor. Sodium carbonate is in a powder form and allows an easier mixing. The pathway to produce sodium silicate from fly ash is illustrated Equation 2.2 where SiO_2 reacts with sodium carbonate (Na_2CO_3) and is converted to Na_2SiO_3 and carbon dioxide (CO_2).

$$SiO_2(s) + Na_2CO_3(s) \longrightarrow Na_2SiO_3(s) + CO_2(g) \qquad \text{Equation 2.2}$$

Temperature is also a very important factor for synthesis. For fly ash where silica source is in amorphous form, the setting reaction temperature must not be too severe, at around 500°C. However, pure crystalline silica like quartz needs a much higher reaction temperature, e.g. above 1400°C, to be able to induce phase changes of the structure (Zhao et al., 2012). However, sodium silicate showed different selectivity, dispersing activity and efficiency depend on the mineral system and silicate dosage (Yang et al., 2008).

Table 2.6 summarizes the literature details on the effect of various factors on the sodium silicate synthesis.

Table 2.6 Sodium silicate Synthesis (Fusion)

Silica source	Alkali source	Fusion				Condition silicate solution		Product	References
		T(°C)	Reaction time	Weight Ratio Silica:Alkali	Remelted	Solvent	Stirred time		
Silica glass	Na_2CO_3	1450	30-45 minutes	1:1	1450 °C, >10min	-	-	Solid product	(Hovis *et al.*, 2004)
		1400	4 hours		1400°C, 2 hours	Deionized water at high temperature and high pressure	19-26 hours	Solution product	(Yamashita *et al.*, 2008)
Silica powder		1500	-	1:1.7	-	-	-	Solid product	(Zhao *et al.*, 2012)
		1700		13:1	-	-	-		
Silica quartz		1450	2 hours	1:1.2	-	Deionized water	-	Solution product	(Ding *et al.*, 2012)
Coal Fly Ash	NaOH	550	1 hour		-		1 day	Solution product	(Halina *et al.*, 2007)
					-	Salt solution	over night	Solution product	(Belviso *et al.*, 2012)
			1.5 hour	1:2	-	Demineralized water	2 hours	Solution product	(Musyoka et al., 2012)
		577	Several hours	1:1.2	-	Deionized water	>1 day	Solution product	(Misran et al., 2007)
Bagasse Fly Ash		500	1 hour		-		2 hours	Solution product	(Purnomo *et al.*, 2012)

CHAPTER 3
MATERIALS AND METHODS

3.1 Materials

- Bagasse fly ash (Black powder)

Figure 3.1 Bagasse fly ash

- Sodium carbonate anhydrous. It has molecular weight of 105.98 grams/mol, chemical formula is Na_2CO_3. (CARLO ERBA, Purity ≥ 99.5%, white powder)

Figure 3.2 Sodium carbonate anhydrous

- Hydrochloric acid 37%

3.2 Sodium silicate synthesis procedure

This work can be briefly summarized as a flow diagram in Figures 3.3.

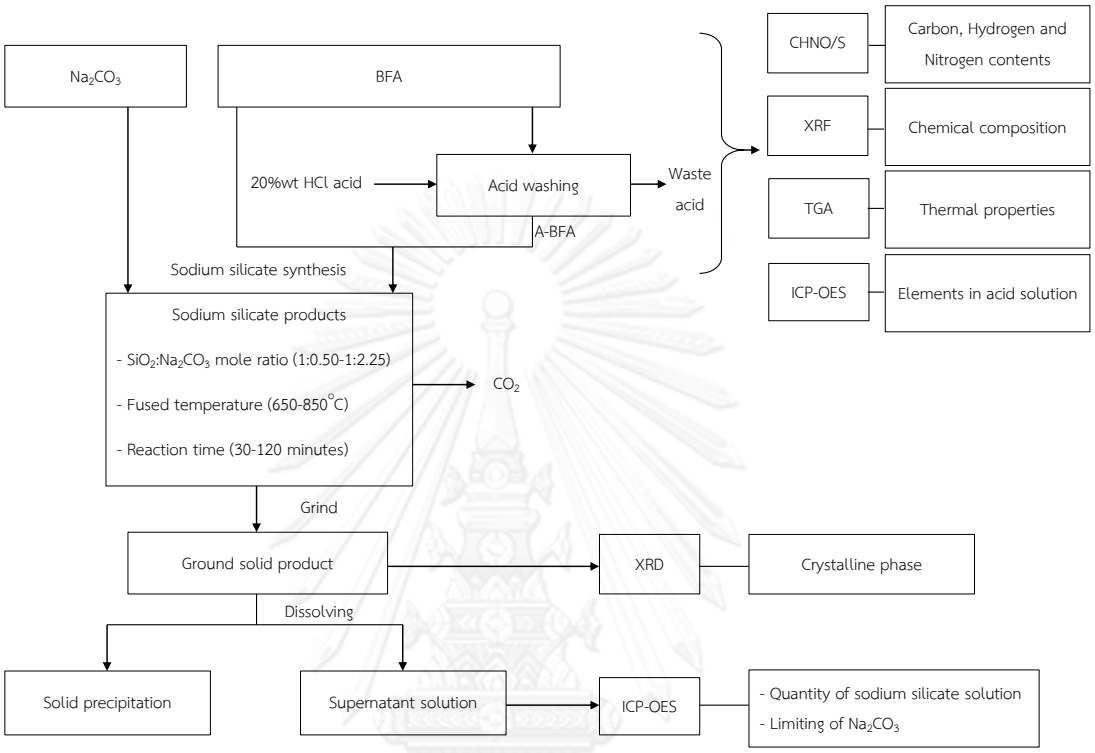

Figure 3.3 Outline of experiments

3.3 Acid washing process

1. Mix 20 grams of original bagasse fly ash with 500 mL of hydrochloric acid solution (20%wt)

2. Heat up the mixture to 80°C and stirred for 2 hours

3. Separate the solid and waste acid solution

4. Dry the acid-bagasse fly ash at 105°C over night

5. Analyse the waste acid solution for elements by ICP-OES

3.4 Thermal process (Sodium silicate synthesis)

3.4.1 Effect of SiO_2:Na_2CO_3 mole ratio

1. Mix 1 mmol SiO_2 (BFA 1 grams or A-BFA 0.82 grams) with 0.50-2.25 mmol Na_2CO_3 in boat crucible

2. Heat up the boat crucible to 830°C (650, 750, 800 and 850°C) and maintain at this temperature for 60 minutes (30 and 120 minutes) in electric furnace

3. Cool down the boat crucible in room temperature (30°C)

4. Weigh the solid product

5. Repeat this section 2 times

3.4.2 Effect of fused temperature

1. Mix 1 mmol SiO_2 (BFA 1 grams or A-BFA 0.82 grams) with Na_2CO_3 at the suitable mole ratio as determined from Section 3.4.1 in boat crucible

2. Heat up the boat crucible to 650, 750, 800, 830 and 850°C for 60 minutes (30 and 120 minutes) in electric furnace

3. Cool down the boat crucible to room temperature (30°C)

4. Weigh the solid product

5. Repeat this section 2 times

จุฬาลงกรณ์มหาวิทยาลัย
Chulalongkorn University

3.4.3 Effect of reaction time

1. Mix 1 mmol SiO_2 (BFA 1 grams or A-BFA 0.82 grams) with Na_2CO_3 at the ratio determined from Section 3.4.1 in boat crucible

2. Heat up the boat crucible to the suitable temperature as determined from Section 3.4.2 for 30-120 minutes in electric furnace

3. Cool down the boat crucible to room temperature (30°C)

4. Weigh the solid product

5. Repeat this section 2 times

3.5 Analysis of solid products

Analyst the ground solid products by XRD diffraction for crystalline phase of sodium silicate, silica and sodium carbonate crystal.

3.5.1 Sodium silicate in supernatant

1. Grind the solid products from Section 3.4

2. Dissolve the solid products 0.4 grams with deionized water 10 mL

3. Separate supernatant solution and solid precipitate

4. Analyse the supernatant solution using ICP-OES to determine the chemical content in supernatant solution such as silicon and sodium elements

3.5.2 Solid precipitate

1. Keep the solid precipitation after dissolving at 105°C for overnight in oven

2. Weigh this solid precipitation

3. Calculate chemical contents in solid product (from the mass balance of elements in raw material and in supernatant solution)

จุฬาลงกรณ์มหาวิทยาลัย
Chulalongkorn University

3.6 Analytical methods

3.6.1 Elemental Analyzer (CHNS/O), Model Perkin Elmer PE 2400 Series II

Carbon, nitrogen and hydrogen contents were analyzed by CHN/O analyzer. The elements were fused at high temperature with excess oxygen.

3.6.2 X–Ray Fluorescence Spectrometer (XRF), Model Philips PW2400

XRF analyzes the amount of each chemical composition. This technique detects the X-ray fluorescence discharged by each element which has specific fluorescent wavelength. Therefore, the analysis shows chemical composition and its quantity in the sample. Before analyzing, the sample is pre-heated to 450°C for remove unburned and volatile carbons compounds.

3.6.3 Thermogravimetric Analyzer (TGA), Model Perkin Elmer TGA 7

The volatile of organic carbon was analyzed thermal decomposition, oxidation or dehydration by weight loss as a function of temperature from 50 to 1000 $^{\circ}$C in nitrogen flow.

3.6.4 X–Ray Diffractometer (XRD), Model Bruker D8-Discover

Property of material is analyzed with X-ray diffraction at 5°-60° with Cu K_{α} radiation for its crystalline structure. Operating with accelerating voltage is 40 kV and 100 mA. This will reflect the sample chemical composition, chemical structure, size of particle and % crystalline.

3.6.5 Inductively Coupled Plasma Optical Emission Spectrometer (ICP-OES), Model Agilent Technology ICP-Plasma-710

Elemental analysis was conducted with atomic spectroscopy by heating up the liquid sample until the atom was broken, atomic plasma or ions were activated and released light at specific wavelength which was measured by detector. The intensity of the wavelength depended on the amount of elements in sample.

CHAPTER 4
RESULTS AND DISCUSSION

4.1. Characterization of bagasse fly ash silica source

4.1.1 Composition of bagasse fly ash (BFA) and acid washed bagasse fly ash (A-BFA)

BFA used in this study is fine moist black powder as shown in Figure 3.1. Its composition was analyzed with CHNS/O and X-ray Fluorescence spectrometer whereas the spent acid after acid washing process was analyzed with ICP–OES as detailed below.

- Analysis of BFA and A-BFA by CHN/O

BFA consisted of 18%wt of carbon, 1%wt of hydrogen, and 0.5%wt of nitrogen whereas A-BFA consisted of 15%wt of carbon, 1%wt of hydrogen, and 0.5%wt of nitrogen. Carbon in A-BFA was lower than that in the original BFA because some carbon was digested by concentrated hydrochloric acid at high temperature ($80^{\circ}C$) during the acid washing process that supported by Zhang *et al.* (2012), Dong *et al.* (2009) and Yin *et al.* (2011).

- Analysis of BFA and A-BFA by XRF instrument

Table 4.1 shows the chemical components of BFA and A-BFA in percentage by weight determined from X-ray Fluorescence. The results presented that silica was the major component of both BFA (63%wt) and A-BFA (77%wt). After acid washing, other elements in BFA decreased from 21 to 5%wt due potentially to the dissolution of such components, e.g. potassium, calcium, sodium, aluminum, iron, in acid solution.

XRF analysis also presented the percentage loss of weight on ignition (%LOI) which was 16%wt of BFA and 18%wt of A-BFA. This was due to the escape of carbon or other organic compounds up on ignition.

- Analysis of spent acid after acid washing process by ICP-OES

ICP-OES results demonstrate that several trace elements were dissolved out of BFA into the acid solution such as potassium, calcium, sodium, aluminum, iron. Similar findings were reported by Iyer (2002). This implied that A-BFA

is a more effective raw material for silicon than BFA as it has higher silicon purity than BFA.

Table 4.1 Elemental Components of BFA, A-BFA, and spent acid solution

Chemical Component	Percentage by weight		
	BFA*	A-BFA*	Spent Acid Solution**
Na_2O	0.349	0.076	0.209
MgO	1.667	0.355	0.739
Al_2O_3	3.668	0.146	2.722
SiO_2	**62.810**	**76.852**	**-**
P_2O_5	2.146	0.280	2.146
SO_3	2.959	1.020	2.959
Cl	0.991	0.763	0.293
K_2O	3.193	1.201	3.143
CaO	3.913	0.376	3.769
TiO_2	0.251	0.198	-
Cr_2O_3	0.026	0.012	-
MnO_2	0.158	0.047	-
Fe_2O_3	1.791	0.347	0.879
NiO	0.007	-	-
ZnO	0.010	-	0.038
SrO	0.005	0.010	-
ZrO_2	0.014	-	-
BaO	0.043	-	-
%LOI	16.415	18.587	-

Remarks: * Analyzed by XRF

** Analyzed by ICP-OES

All samples were dried at 105°C.

%LOI=%Loss on Ignition

จุฬาลงกรณ์มหาวิทยาลัย
Chulalongkorn University

4.1.2 Thermal analysis

Figure 4.1 illustrates the weight change as a function of temperature under nitrogen flow. Total weight losses of BFA and A-BFA silica source were 12% and 5%, respectively. Virtually, volatile organic compounds in BFA and A-BFA silica sources were decomposed in two temperature zones. The first zone occurred at the temperature range between 250 and 480°C where the weight losses for BFA and A-BFA were 1% and 0.5%. According to Batra *et al.* (2008), the decomposed contents at this temperature were hydroxide compounds or moisture.

The second zone was at the temperature above 480°C where the major weight loss occurred. The weight losses of BFA and A-BFA were 11% and 5%, respectively. Both BFA and A-BFA showed similar trend of weight loss, i.e. the loss of weight occurred steadily at this temperature range without any ramps. This could be because the decomposed contents of the two sources were of the same nature, i.e. the same volatile organic functional groups. However, the loss of weight of A-BFA was smaller than that of BFA as most of the decomposable components in A-BFA were removed during the acid washing process.

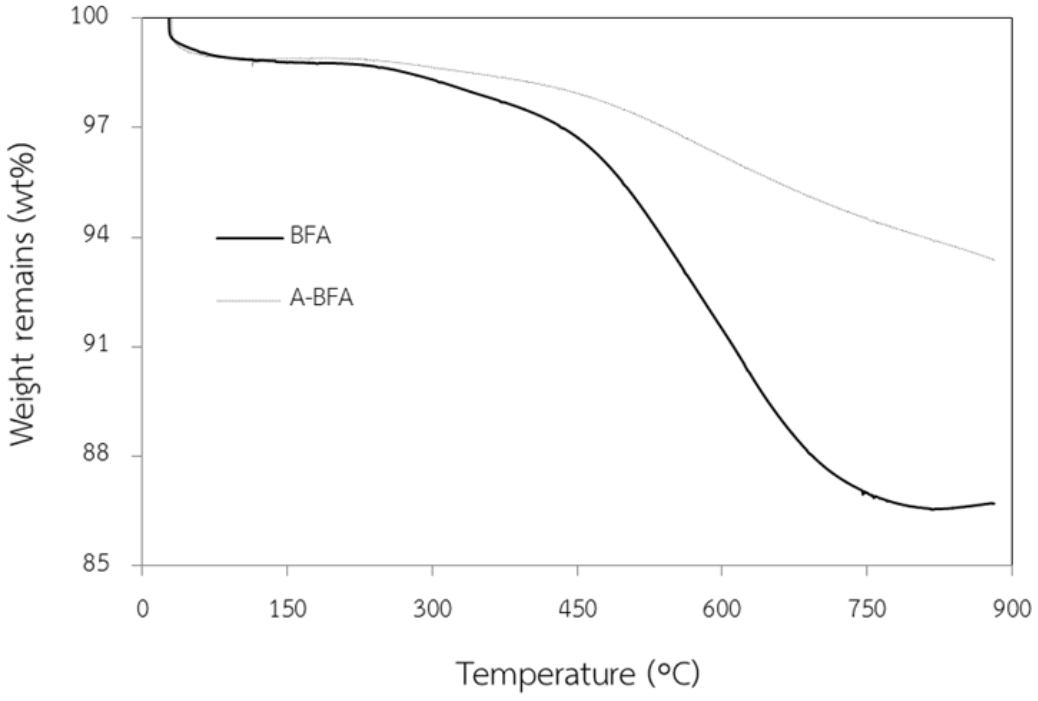

Figure 4.1 TGA analysis of raw materials

4.1.3 Structure analysis

The XRD diffraction pattern of BFA raw material was matched with the database in the Joint Committee on Powder Diffraction Standard (JCPDs) as displayed in Figure 4.2. Most BFAs showed low crystalline phase of quartz-SiO_2 (no. 01-083-0539). BFA stored in a furnace at very high temperature, i.e. 950°C, presented the formation of cristobalite-SiO_2 (01-082-0512) structure which is a highly stable form of SiO_2 and is not the target form for this work. From this result, the fused temperature should be lower than 950°C.

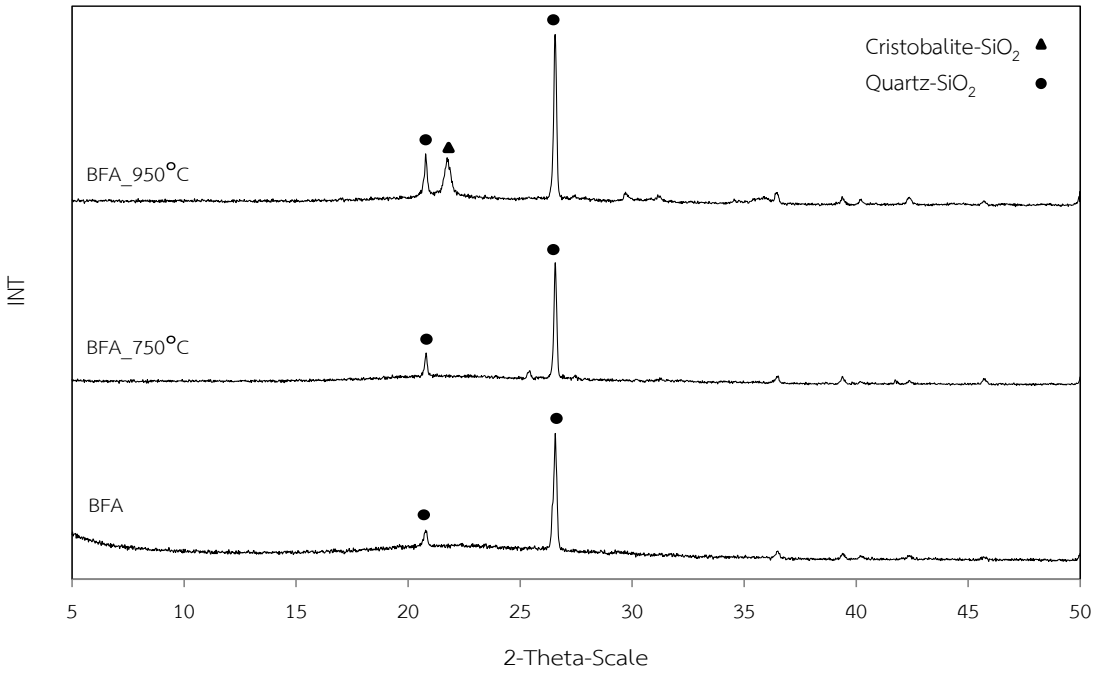

Figure 4.2 XRD diffraction patterns of raw materials

จุฬาลงกรณ์มหาวิทยาลัย
CHULALONGKORN UNIVERSITY

4.2 Sodium silicate production

4.2.1 Effect of ratio of SiO_2:Na_2CO_3 on the formation of sodium silicate

In this experiment, the fused products from BFA and A-BFA were dissolved in deionized water and the concentration of sodium silicate in the solution (soluble Na_2SiO_3) was measured with ICP-OES whereas the remaining solid insoluble was analyzed for its crystal composition with XRD. Insoluble sodium silicate was analyzed by mass balance as both SiO_2 and Na_2CO_3 are the two major raw materials for the formation of sodium silicate. The solid product was weighed both before and after synthesis step. Note that in Appendix B, the optimal condition for the synthesis was selected from the temperature range of 650-850°C and reaction time of 30-120 minutes where the optimal condition occurred at 830°C for 60 minutes.

Figures 4.3 a (BFA) and 4.3 b (A-BFA) present the mass of soluble sodium silicate, insoluble sodium silicate in the solid products at different initial SiO_2:Na_2CO_3 mole ratios. Soluble sodium silicate was analyzed for concentrations of silicon and sodium elements. The other components such as sodium carbonate (Na_2CO_3), silica quartz (SiO_2), insoluble sodium silicate and metal oxide or other compounds were estimated by residual elements from mass balance. Increasing Na_2CO_3 was shown to have positive effect on the formation of sodium meta-silicate solution (soluble Na_2SiO_3), where in this work this will be called, otherwise stated, as soluble sodium silicate, and insoluble sodium silicate especially at low ratio of SiO_2:Na_2CO_3 (1:0.75-1:1.25). A further increase in total sodium silicate (Na_2SiO_3) did not seem to give additional effect on the formation of total sodium silicate (Na_2SiO_3). This figure presents that soluble sodium silicate and insoluble sodium silicate reached constant level when Na_2CO_3 in the SiO_2:Na_2CO_3 was higher than 1.25. The maximum soluble sodium silicate was 0.007 and 0.008 mmol for fused products from BFA and A-BFA, respectively, whereas insoluble sodium silicate was 0.004 and 0.003 mmol, respectively.

In the solid products, the results demonstrate that more silica was consumed when more sodium carbonate was added to the system. Increasing the content of sodium carbonate beyond the SiO_2:Na_2CO_3 mole ratio of 1:1.00 and 1:1.25 (for BFA and A-BFA) saw a remnant of sodium carbonate remaining in the product, which indicates that there was an excess of sodium carbonate for the reaction. Thus, it was set as a reference in this work that a larger fraction of Na_2CO_3 in the SiO_2:Na_2CO_3 mole ratio than 1:1.25 presented an excess sodium source. The formation of total sodium silicate (Na_2SiO_3) with the various raw material ratio is demonstrated in Figure

4.3 which indicated that soluble sodium silicate (soluble Na_2SiO_3) increased with the increase in Na_2CO_3 up to a certain concentration level that most SiO_2 was react after which a further increase in Na_2CO_3 did not further enhance the formation of total sodium silicate (Na_2SiO_3). This occurred when SiO_2:Na_2CO_3 mole ratio reached 1:1.75 for both BFA and A-BFA sources.

จุฬาลงกรณ์มหาวิทยาลัย
Chulalongkorn University

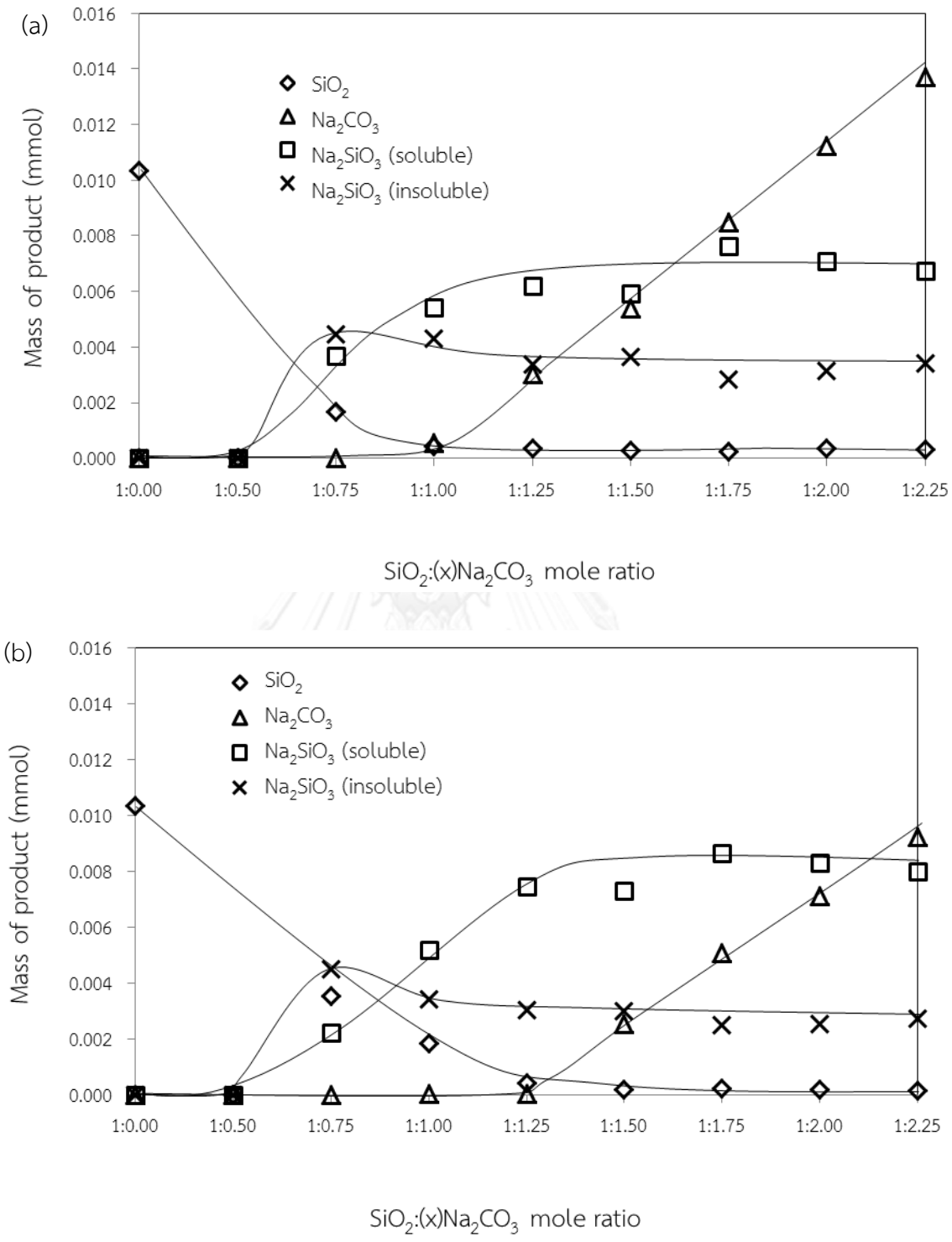

Figure 4.3 Mass of products from BFA (a) and A-BFA (b) at various mole ratios of SiO_2:(x)Na_2CO_3 (830°C fused temperature, 60 minutes reaction time)

Yields of soluble and insoluble sodium silicates were observed for both BFA (Figure 4.4 a) and A-BFA (Figure 4.4 b). Mass balances of this reaction could be summarized as shown in Figure 4.4, where the mass of solid product was compared with its precursor at the same synthetic condition which allowed the estimates of the yield of total sodium silicate. From this figure, it can be seen that adding more sodium source as a raw material (Na_2CO_3 in this case) increased the yield of the reaction both for BFA and A-BFA, but would lead to a smaller fraction of silica product (total sodium silicate) as Na_2CO_3 was also remained in the product mixture (insoluble Na_2SiO_3).

The maximum yield of soluble and insoluble sodium silicates was presented at 1:1.25 of SiO_2:Na_2CO_3 mole ratio where the soluble/insoluble yields were 35%/18% and 47%/19% for BFA and A-BFA, respectively.

The results indicate that SiO_2 in A-BFA was used more effectively than SiO_2 in BFA. This could be due to the fact that SiO_2 in A-BFA was being better distributed in the raw materials which could react more easily with Na_2CO_3. According to Karlfeldt Fedje et al. (2010), the acid treatment could enhance the surface properties of the raw material which might well explain the findings in this work.

จุฬาลงกรณ์มหาวิทยาลัย
Chulalongkorn University

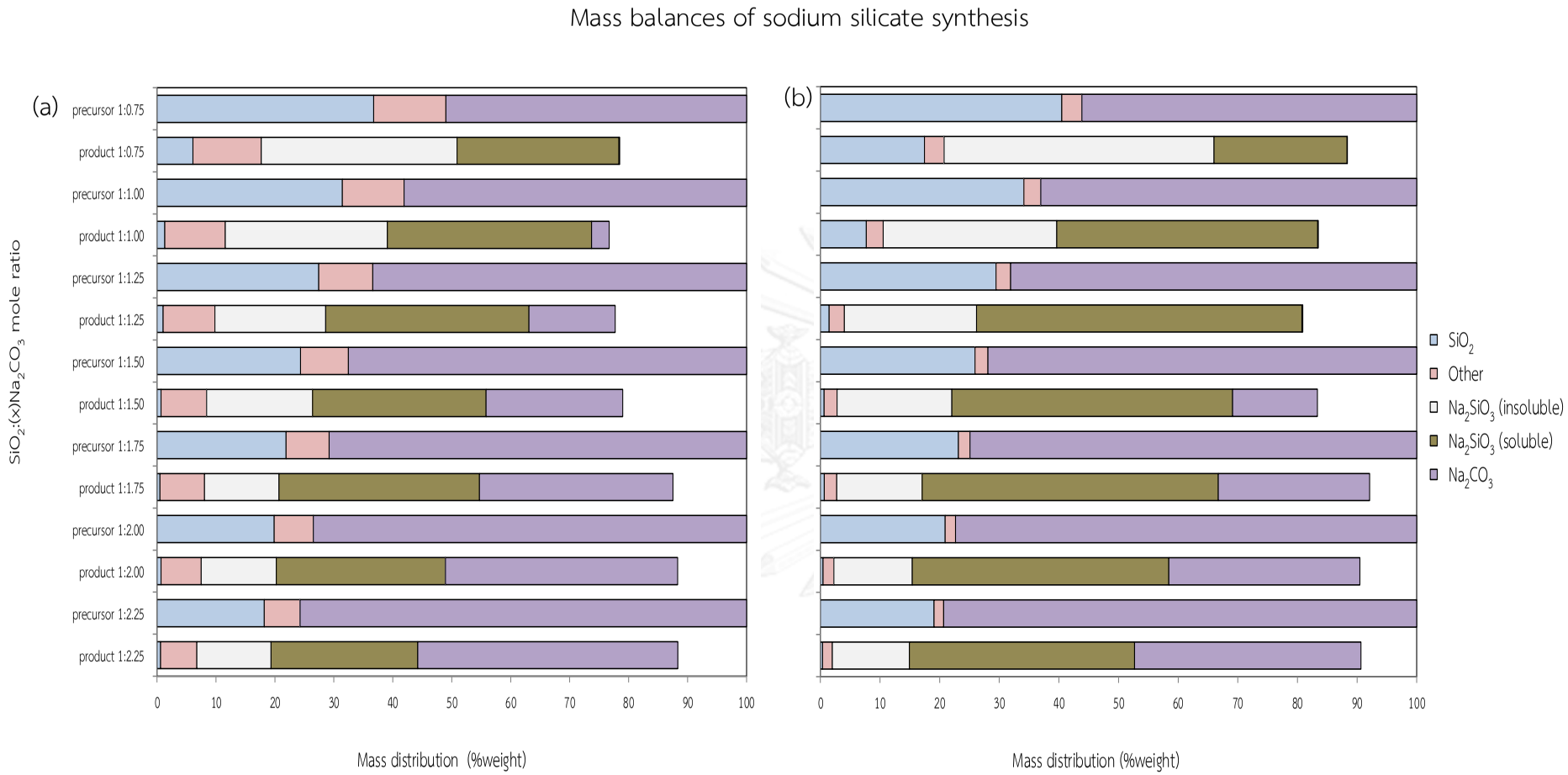

Figure 4.4 Mass distribution of various components in the fused products from BFA (a) and A-BFA (b) at various mole ratios of SiO_2:(x)Na_2CO_3 calculated base on total mass of raw materials for each condition (830°C fused temperature, 60 minutes reaction time)

Figure 4.5 is the XRD diffraction patterns of total sodium silicate (Na_2SiO_3) in the solid products obtained from BFA and A-BFA raw materials. This revealed that the SiO_2:Na_2CO_3 mole ratio in the range from 1:0.75 to 1:1.75 for BFA source and 1:1.50 to 1:1.75 for A-BFA source led to a formation of the crystalline phase of total sodium silicate (Na_2SiO_3) as the major structure in the solid products for BFA (in Figure 4.3 a) and A-BFA (in Figure 4.3 b). The crystalline phase of total sodium silicate (Na_2SiO_3) structure increased with the decrease in SiO_2:Na_2CO_3. All solid products exhibited quartz-SiO_2 peak, and at the mole ratio lower than 1:1.00 (high Na_2CO_3), an additional phase of Na_2CO_3 was also observed which suggested a much too high level of Na_2CO_3 in the raw material. A close comparison between the product diffraction pattern from the two raw material sources, i.e. BFA and A-BFA, demonstrated that quartz-SiO_2 peak was only observed in the product derived from BFA and not A-BFA (at SiO_2:1.50Na_2CO_3). This suggested that the quartz crystal in A-BFA might have been converted to the form that could be reacted more easily with Na_2CO_3. Therefore this led to a greater formation of soluble sodium silicate (soluble Na_2SiO_3) in the product (as per unit of raw material) as shown in Figure 4.4.

In addition, at this condition (1:1.50), there were the crystals of total Na_2CO_3 formed in the remaining solid products indicating an excess of CO_3^{2-} for the reaction. An increase in Na_2CO_3 saw a decrease in the remaining SiO_2 until SiO_2:Na_2CO_3 was below 1:1.25 where SiO_2 was almost totally reacted.

It was worth noting here that the composition of the solid precipitate after the reaction was estimated from the mass balances of the various compositions along with the results from XRD analysis which helped identify some of the remaining crystals in the solid structure.

In this reaction, the silica raw materials contained one molecule of Si^{4+} and four O^{2-}, which form tetrahedral structure and sometimes this was arranged in quartz framework. This SiO_2 and quartz were opened by alkali treatment where sodium was incorporated and rearranged the new tetrahedral structure of silica in which O^{2-} and Na^{+} formed new silicate compounds as presented by the chemical formulae of Na_2SiO_3. Na_2SiO_3 is well-known single chain silicate but various combination of sodium silicate structure could be formed depending on the synthetic conditions.

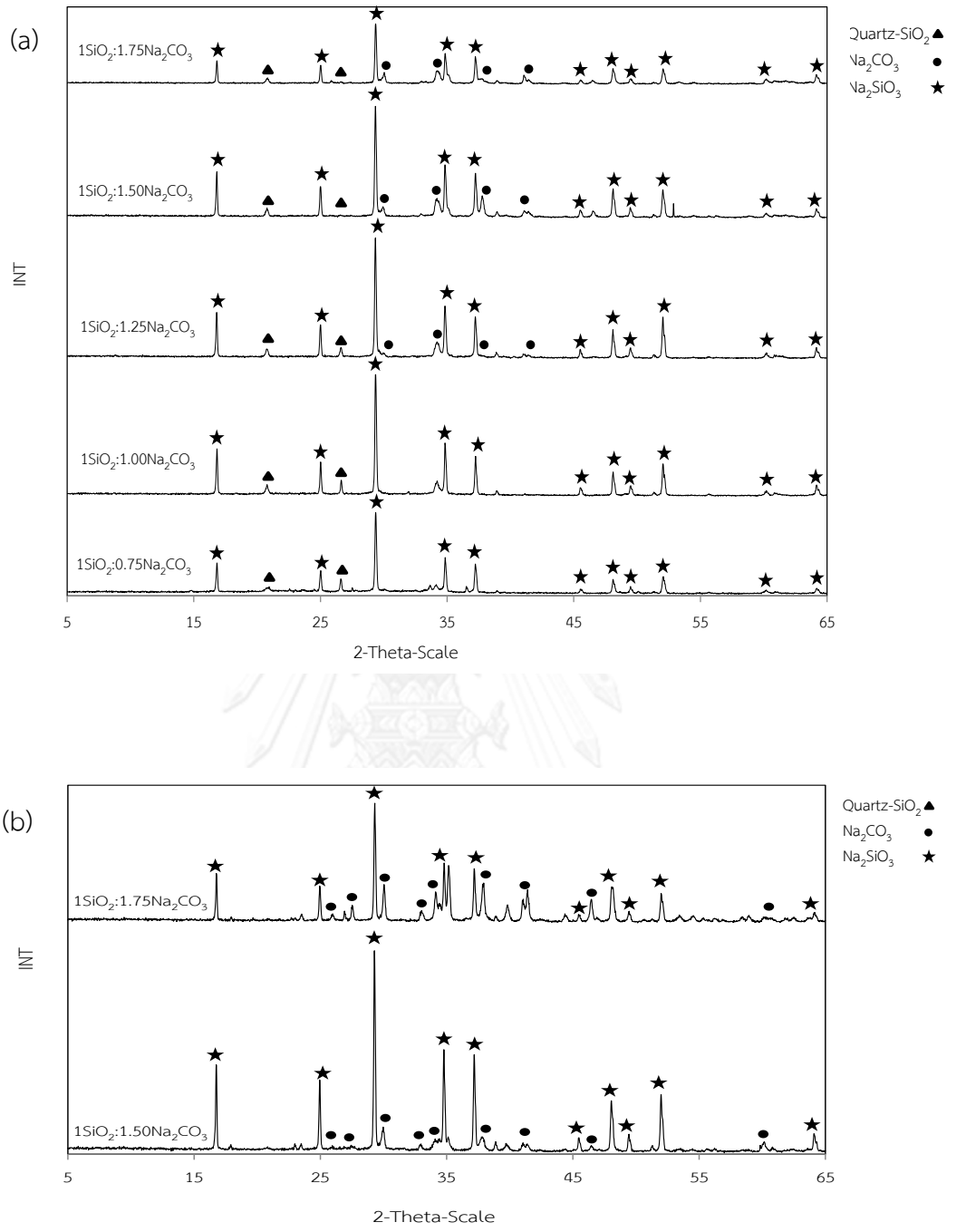

Figure 4.5 XRD diffraction patterns of BFA (a) and A-BFA (b) products at various mole ratios of SiO_2:(x)Na_2CO_3 (830°C fused temperature, 60 minutes reaction time)

4.2.2 Effect of fused temperature on sodium silicate production

In this section, the experiments were conducted to find suitable temperature for the fused reaction while the other conditions were maintained at the optimal as determined from the previous section.

Figure 4.6 a (BFA) and 4.6 b (A-BFA) presents mass of soluble sodium silicate, insoluble sodium silicate in the solid products at different fused temperatures (650, 750, 800, 830 and 850°C). Soluble sodium silicate was analyzed for concentrations of silicon and sodium elements. The other components such as quartz silica (SiO_2), insoluble sodium silicate (insoluble Na_2SiO_3) and metal oxide or other compounds were estimated by residual elements from mass balance. Increasing fused temperature was shown to have positive effect on the formation of soluble sodium silicate (soluble Na_2SiO_3) mainly at high fused temperature (830-850°C). A further increase in fused temperature did not seem to give additional effect on the formation of soluble sodium silicate (soluble Na_2SiO_3). This figure illustrates that a constant weight of soluble and insoluble sodium silicates were obtained at the fused temperature higher than 830°C. The maximum soluble sodium silicate was 0.006 and 0.008 mmol for fused products from BFA and A-BFA, respectively, whereas insoluble sodium silicate was 0.004 and 0.003 mmol, respectively. Note that the product from the reaction at higher fused temperature than 850°C melted and fused with the boat crucible, and cannot be separated from the crucible. At temperature higher than 800°C, more soluble sodium silicate was formed whilst a decrease in insoluble sodium silicate was observed. This suggests that a better reaction might have occurred as more silica and sodium carbonate were also consumed at this high temperature resulting in a decreasing level of silica and sodium carbonate in the solid product.

The formation of total sodium silicate (Na_2SiO_3) with the various fused temperature is demonstrated in Figure 4.6 which indicated that soluble sodium silicate (soluble Na_2SiO_3) increased with an increase in fused temperature while insoluble sodium silicate (insoluble Na_2SiO_3) was decreased. The fused temperature was affected to form of sodium silicate synthesis. Data in this figure were obtained from the mass balances of elements. It can be seen that metal oxides or other compounds remained constant throughout the temperature range which is logical as they did not involve in the reaction. SiO_2, on the other hand, entered the reaction in a greater extent at high temperature, and particularly at temperature higher than 800°C. That is why there was a drastic drop in the concentration of SiO_2 at 800°C.

Due to this reason, it was anticipated that total sodium silicate (Na_2SiO_3) would increase steadily with temperature which was observed and described in the previous paragraph. However, in the solid precipitate, insoluble sodium silicate dropped slightly at 750°C and restored the high concentration at higher temperature. This might be attributed to the different forms of sodium silicates such as $Na_2Si_2O_5$ which might have taken place at this temperature and this was not dissolved well in water.

In conclusion, sodium silicate reaction seemed to have endothermic nature as increasing fused temperature resulted in an increasing reaction extent.

จุฬาลงกรณ์มหาวิทยาลัย
Chulalongkorn University

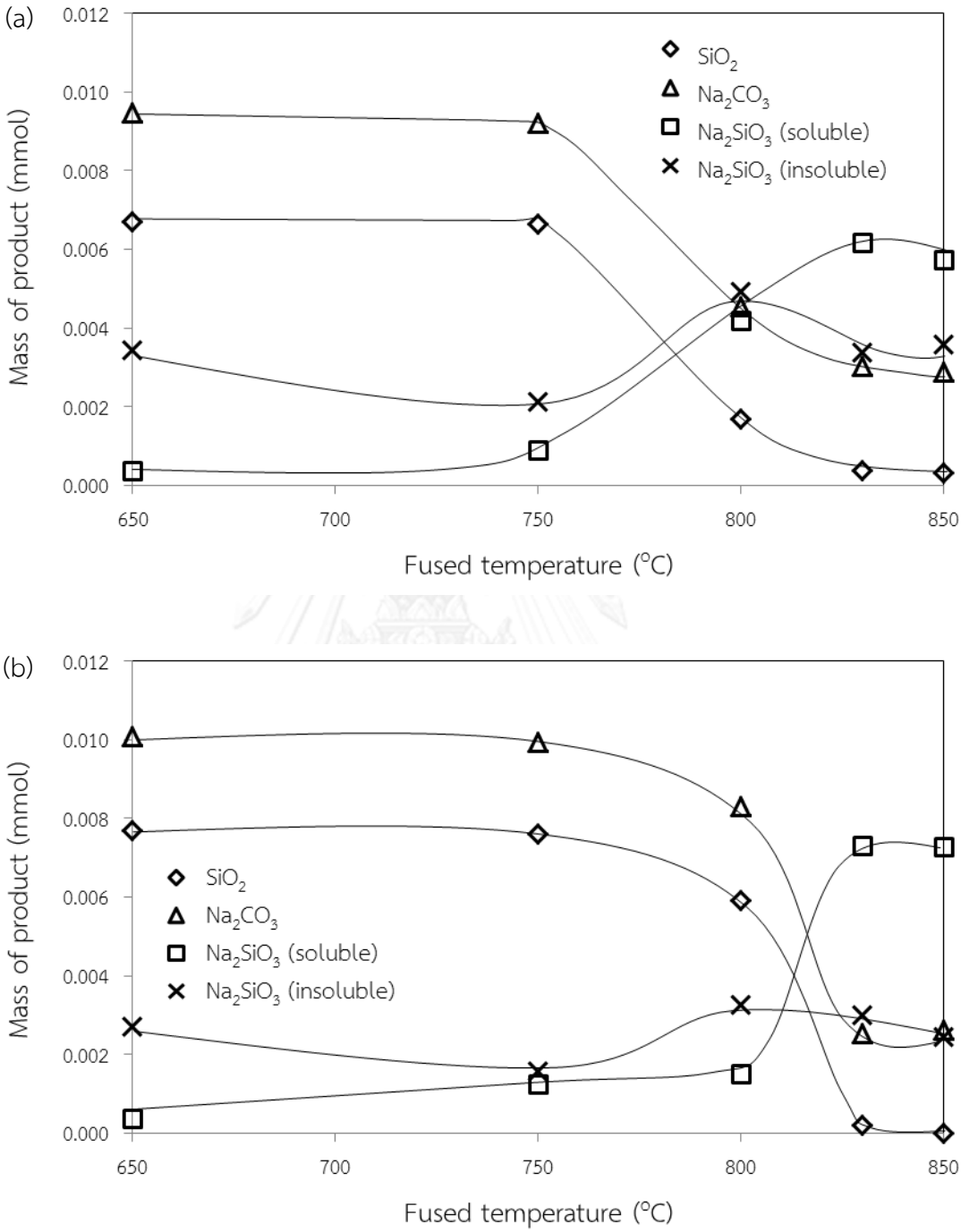

Figure 4.6 Mass of products from BFA (a) and A-BFA (b) at various fused temperatures (SiO_2:1.25Na_2CO_3 mole ratio, 60 minutes reaction time)

This figure illustrates that increasing fused temperature enhanced the yield of the reaction both for BFA and A-BFA. The formation of Na_2SiO_3 with various fused temperature is demonstrated in Figure 4.7 which shows that Na_2SiO_3 increased with the increase in fused temperature up to 830^{o}C which is a level that most SiO_2 reacted after which increasing fused temperature did not further enhance the formation of Na_2SiO_3. At this temperature, the maximum yields of soluble and insoluble sodium silicates were 35%/18% and 47%/19% for BFA and A-BFA, respectively.

Figure 4.7 also demonstrates that A-BFA source provided a higher mass of soluble sodium silicate (soluble Na_2SiO_3) than BFA. This could be because SiO_2 in A-BFA was acid-pretreated into a form which is more ready for fused reaction (TAN & WANG, 2009). The results also indicate that acid pretreatment might have converted SiO_2 into a form that is more easily reacted with Na_2CO_3 leading to a greater reaction extent of A-BFA.

จุฬาลงกรณ์มหาวิทยาลัย
Chulalongkorn University

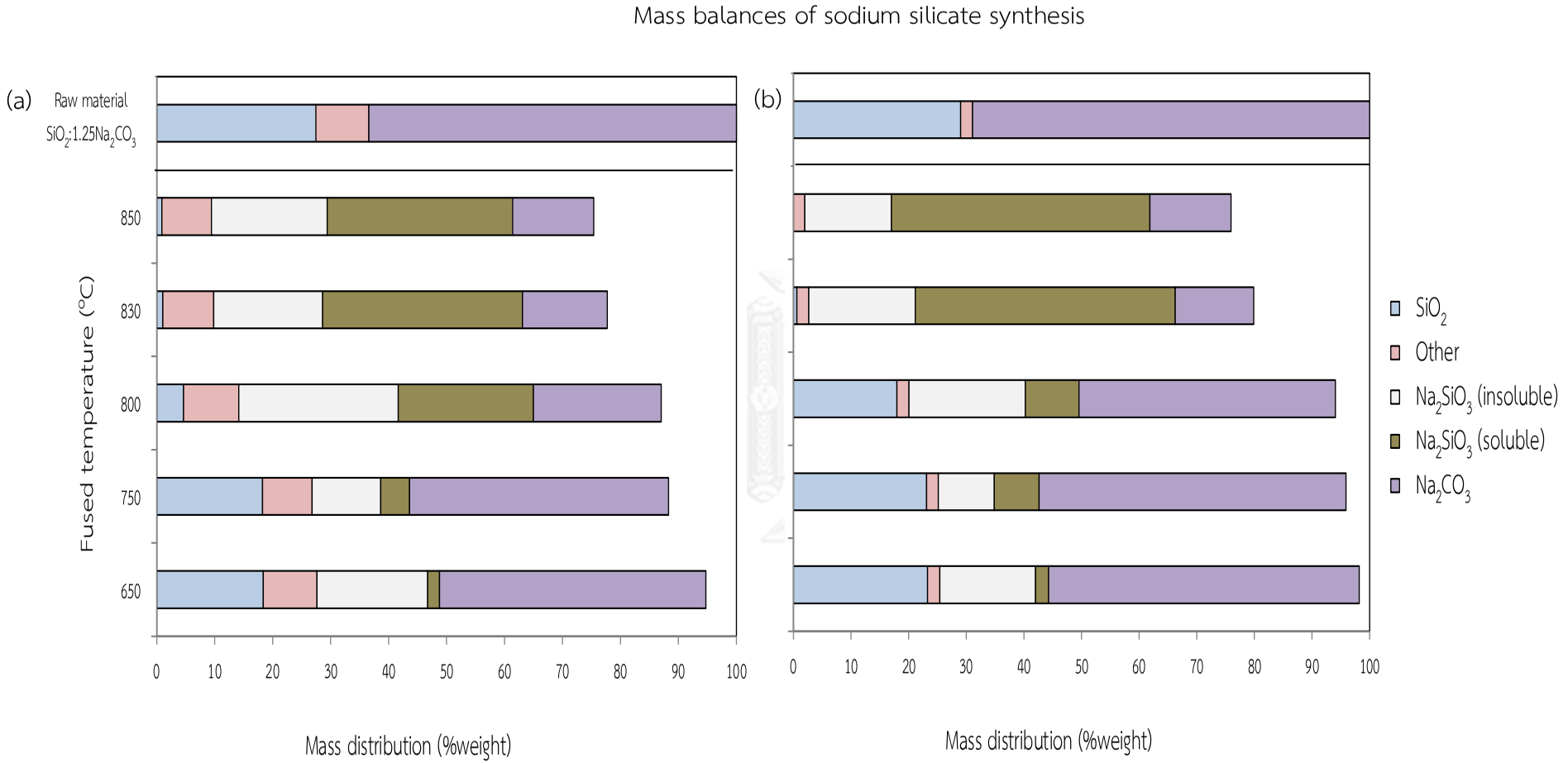

Figure 4.7 Mass distribution of various components in the fused products from BFA (a) and A-BFA (b) at various fused temperature calculated base on total mass of raw materials (SiO_2:1.25Na_2CO_3 mole ratio, 60 minutes of reaction time)

XRD results indicated that there existed other forms of total sodium silicates and this will be discussed in the following paragraph. In addition, XRD results in Figure 4.8 illustrate that, at this condition (830-850^{o}C), there were crystals of SiO_2 and Na_2CO_3 formed in the remaining solid products for BFA source when compared with the product obtained at 800^{o}C. This indicated that a better reaction was obtained at high temperature. Similar findings were observed for both BFA (Figure 4.6 a) and A-BFA (Figure 4.6 b), the difference was that a higher quantity of soluble sodium silicate (soluble Na_2SiO_3) was obtained from A-BFA.

XRD diffraction patterns of sodium silicate products with various fused temperatures are presented in Figures 4.8 for BFA raw materials. This showed that the fused temperature in the range from 800 to 850^{o}C led to a formation of the crystalline phase of total sodium silicate (Na_2SiO_3). The solid products were analyzed with JCPDs patterns of quartz-SiO_2 (01-083-0539), Na_2CO_3 (00-037-0451) and Na_2SiO_3 (00-037-0451), and disodium phyllo-silicate-α-$Na_2Si_2O_5$ (01-076-0707) structures. At the fused temperature of 800^{o}C, a crystalline phase with high quartz-SiO_2, low Na_2CO_3, total sodium silicate (Na_2SiO_3) and $Na_2Si_2O_5$ structures was formed, while increasing the fused temperature to 830 and 850^{o}C led to a formation of a crystalline phase with high Na_2SiO_3, low quartz-SiO_2 and low Na_2CO_3 structures. The crystalline phases of quartz-SiO_2 and Na_2CO_3 decreased with an increase in fused temperature, while the phase of total sodium silicate (Na_2SiO_3) structure increased in solid products (above 830^{o}C). This finding supports the report from Cruz *et al.* (2006) who presented that more silicate product was obtained at higher temperature. It is noticed that the crystalline phase of $Na_2Si_2O_5$ did not appear at the fused temperature above 830^{o}C.

In terms of silicate structure, this section described that fused temperature had a great effect on the formation of silicate structure. At low reaction (800^{o}C), the silicate framework has been transformed from silica in raw material to sheet silicates ($Si_2O_5^{2-}$) and single chain silicates (SiO_3^{2-}), while at high reaction (830 and 850^{o}C), only single chain silicates (SiO_3^{2-}) was obtained.

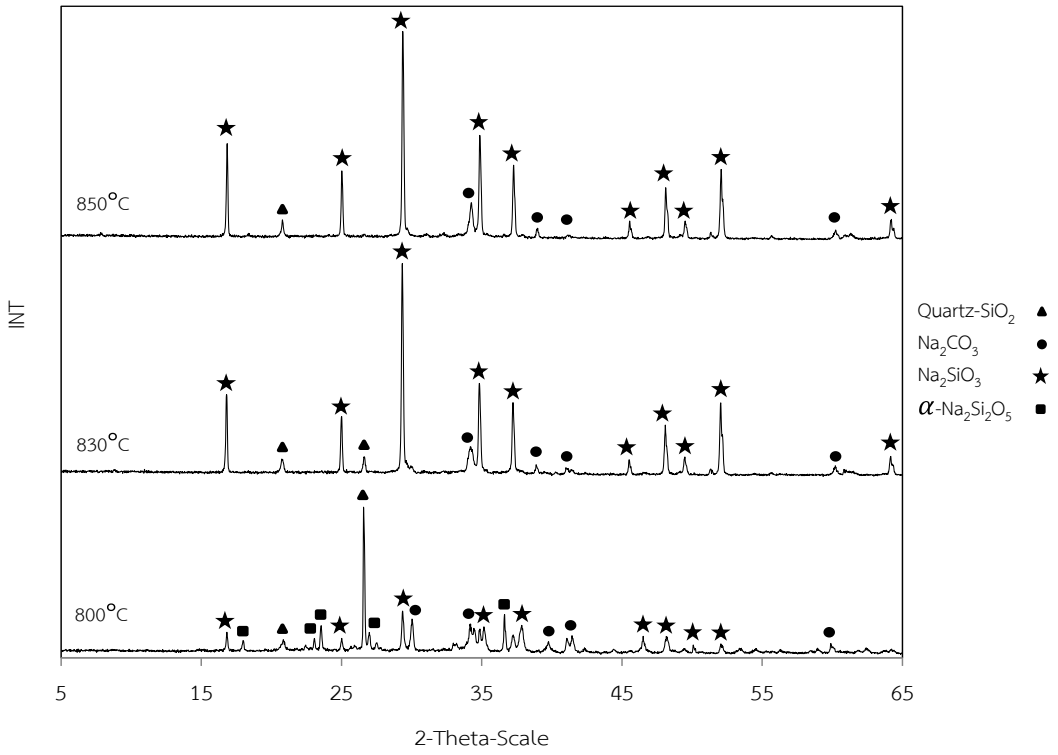

Figure 4.8 XRD diffraction patterns the solid products from BFA at various fused temperature (SiO_2:1.25Na_2CO_3 mole ratio, 60 minutes reaction time)

จุฬาลงกรณ์มหาวิทยาลัย
Chulalongkorn University

4.2.3 Effect of reaction time on sodium silicate production

To investigate the effect of time on the sodium silicate reaction according to Equation 2.2, it was proposed that the reaction temperature was set at 830^{o}C and SiO_2:Na_2CO_3 of 1:1.25 to ensure that the reaction could go to completion. Figure 4.9 displays the mole of soluble sodium silicate (soluble Na_2SiO_3) at different reaction times (30, 60 and 120 min). At 30 min, there still existed a large quantity of SiO_2 in the solid product which indicated that the reaction had not reached completion. Reaction seemed to complete within 60 min when a further increase in reaction time did not seem to have effect on reaction. A much too long reaction time such as 120 min seemed to lower the quantity of Na_2SiO_3 as a subsequent sintering reaction might take place and lowered the yield of soluble sodium silicate (soluble Na_2SiO_3) product.

Figures 4.9 a and 4.9 b illustrate that A-BFA provided a higher mass of soluble sodium silicate (soluble Na_2SiO_3) in the supernatant solution than BFA source. The maximum soluble sodium silicate showed at 60 min that was 0.006 and 0.0075 mmol for BFA and A-BFA source, respectively. Insoluble sodium silicate (insoluble Na_2SiO_3) decreased with increasing reaction time from 30 to 120 min. The formation of Na_2SiO_3 with the various reaction time is demonstrated in Figure 4.9 which indicated that soluble sodium silicate (soluble Na_2SiO_3) increased with the increase in reaction time up to a certain concentration level that most SiO_2 was react after which a further increase in Na_2CO_3 did not further enhance the formation of soluble sodium silicate (soluble Na_2SiO_3). This occurred when reaction time reached 60 minutes for both BFA and A-BFA sources.

จุฬาลงกรณ์มหาวิทยาลัย
Chulalongkorn University

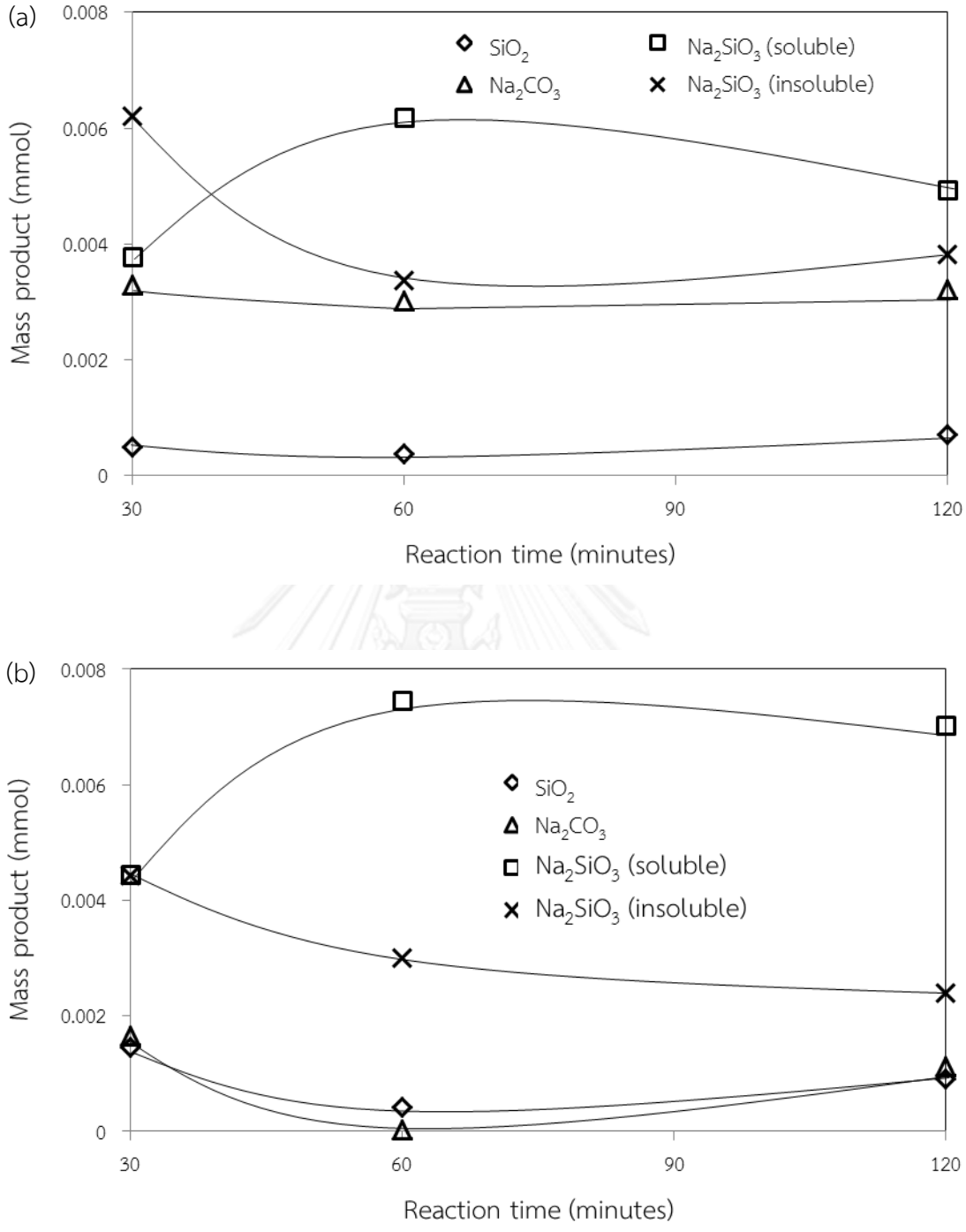

Figure 4.9 Mass of products from BFA (a) and A-BFA (b) at various reaction times (SiO_2:1.25Na_2CO_3 mole ratio, 830°C of fused temperature)

Yields of the soluble sodium silicate were observed for both BFA (Figure 4.10 a) and A-BFA (Figure 4.10 b). From this figure, the maximum yield of soluble and insoluble sodium silicate was presented at 60 min where the soluble/insoluble yields were 35%/18% and 45%/18% for products from silica source of BFA and A-BFA, respectively.

จุฬาลงกรณ์มหาวิทยาลัย
Chulalongkorn University

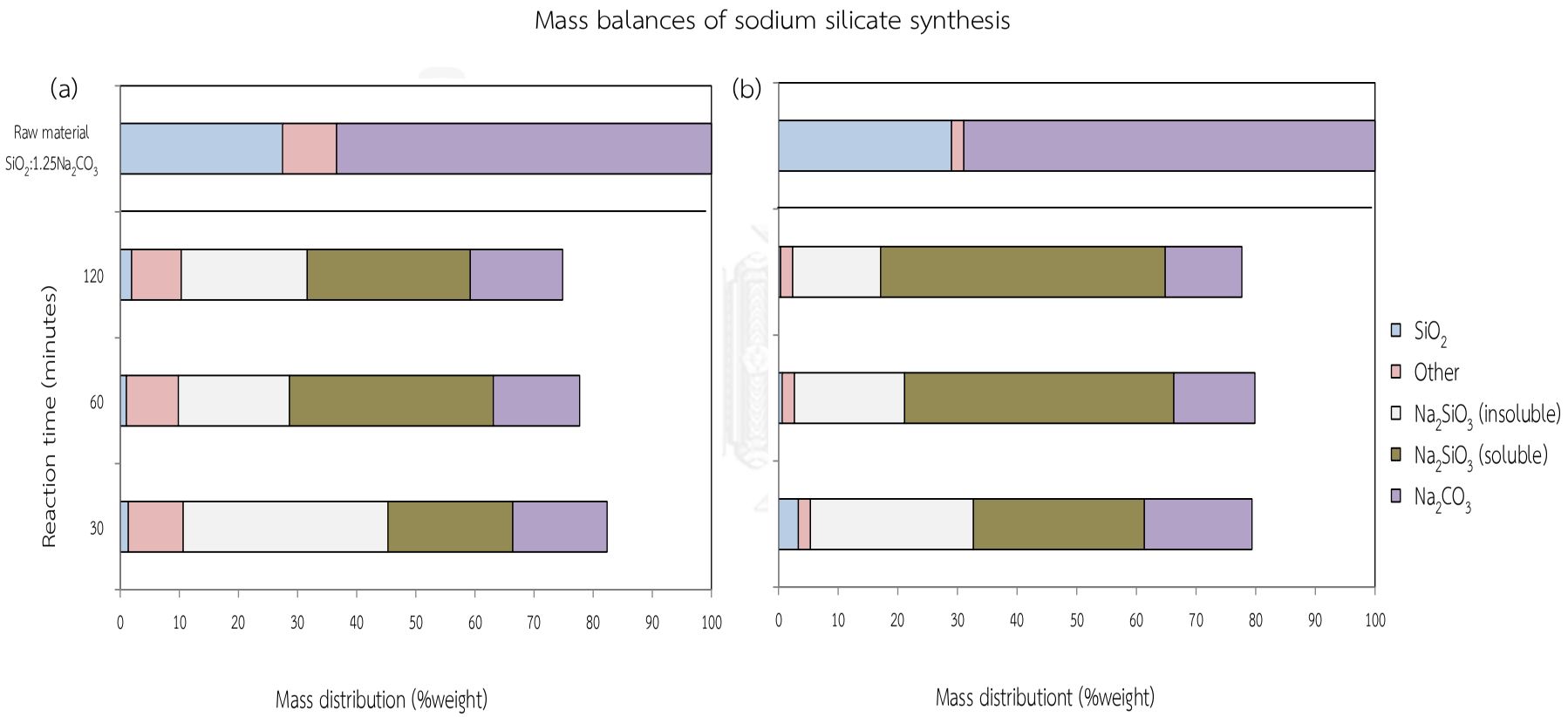

Figure 4.10 Mass distribution of various components in the fused products from BFA (a) and A-BFA (b) at various reaction time calculated base on total mass of raw materials (SiO_2:1.25Na_2CO_3 mole ratio, 830^{o}C of fused temperature)

XRD patterns in Figures 4.11 show that, at 30 min, there existed the crystals of quartz-SiO_2 in the remaining solid product. This quartz disappeared as the reaction increased as it was converted to sodium silicate. The solid products were analyzed with JCPDs patterns of quartz-SiO_2 (01-083-0539), Na_2CO_3 (00-037-0451) and Na_2SiO_3 (00-037-0451), and disodium phyllo-silicate-α-$Na_2Si_2O_5$ (01-076-0707) structures.

Figure 4.11 also illustrates that $Na_2Si_2O_5$ formed at low reaction time, i.e. at 30 min, crystalline phases of high quartz-SiO_2, Na_2CO_3, total sodium silicate (Na_2SiO_3) and low $Na_2Si_2O_5$ were formed. Increasing reaction time to 60 min reduced the quantity of $Na_2Si_2O_5$ and only crystalline phases of total sodium silicate (Na_2SiO_3) and low quartz-SiO_2 were observed. This led to a possible reaction mechanism as proposed here below Equations 4.1-4.3:

$$Na_2CO_3 + 2SiO_2 \rightarrow Na_2Si_2O_5 + CO_2 \qquad \text{Reaction I} \qquad \text{Equation 4.1}$$

$$Na_2CO_3 + SiO_2 \rightarrow Na_2SiO_3 + CO_2 \qquad \text{Reaction II} \qquad \text{Equation 4.2}$$

$$Na_2Si_2O_5 + Na_2CO_3 \rightarrow Na_2SiO_3 + CO_2 \qquad \text{Reaction III} \qquad \text{Equation 4.3}$$

This explained why $Na_2Si_2O_5$ was observed during the early stage of the reaction and disappeared when the reaction went to completion.

From the finding in this work, it can be concluded that the extent of reaction of silica to sodium silicate was controlled significantly by the extent of reaction. The silicate structure framework as silica in the raw material was changed to sodium silicates in two major forms, sheet silicates ($Si_2O_5^{2-}$) at low reaction extent, and single chain silicate (SiO_3^{2-}) at high reaction extent. High reaction extent occurred at relatively high temperature (greater than 830°C) and high reaction time (greater than 60 min).

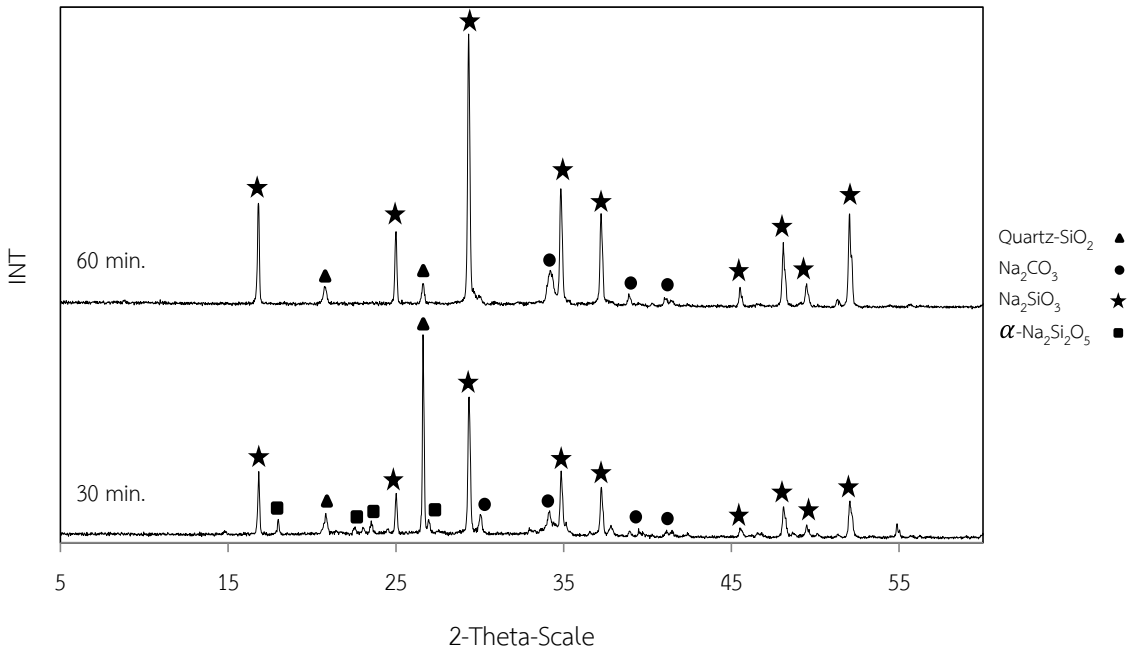

Figure 4.11 XRD diffraction patterns the solid products from BFA at various reaction times (SiO_2:1.25Na_2CO_3 mole ratio, 830°C of fused temperature

จุฬาลงกรณ์มหาวิทยาลัย
Chulalongkorn University

4.3 Polymerization of sodium silicate soluble

Figure 4.12 illustrates the stability of sodium silicate products from BFA and A-BFA. Fresh soluble sodium silicate from BFA has green color due to the existence of some metal oxide impurities, whereas that from A-BFA is transparent. The green color faded away slowly and the solution turned orange 30 days after the synthesis whilst the solution from A-BFA still remained unchanged. This change in color must have been due to some post-reactions of sodium silicate such as the polymerization of silica. Lucas *et al.* (2011), Gaggiano et al. (2011) and Guo et al. (2010) suggested that polysilicate anions or colloids could be polymerized to silanol groups according to Equation 4.4. Polycondensation reaction of silanol could also follow as presented in Equation 4.5 and this mechanistic pathway is illustrated in Figure 4.13.

$$Na_2OSiO_2 + 2H_2O \rightarrow Si(OH)_4 + 2Na^+ + OH^- \quad \text{Equation 4.4}$$

$$(OH)_3Si\text{-}OH + OH\text{-}Si(OH)_3 \rightarrow (OH)_3Si\text{-}O\text{-}Si(OH)_3 + H_2O \quad \text{Equation 4.5}$$

จุฬาลงกรณ์มหาวิทยาลัย
Chulalongkorn University

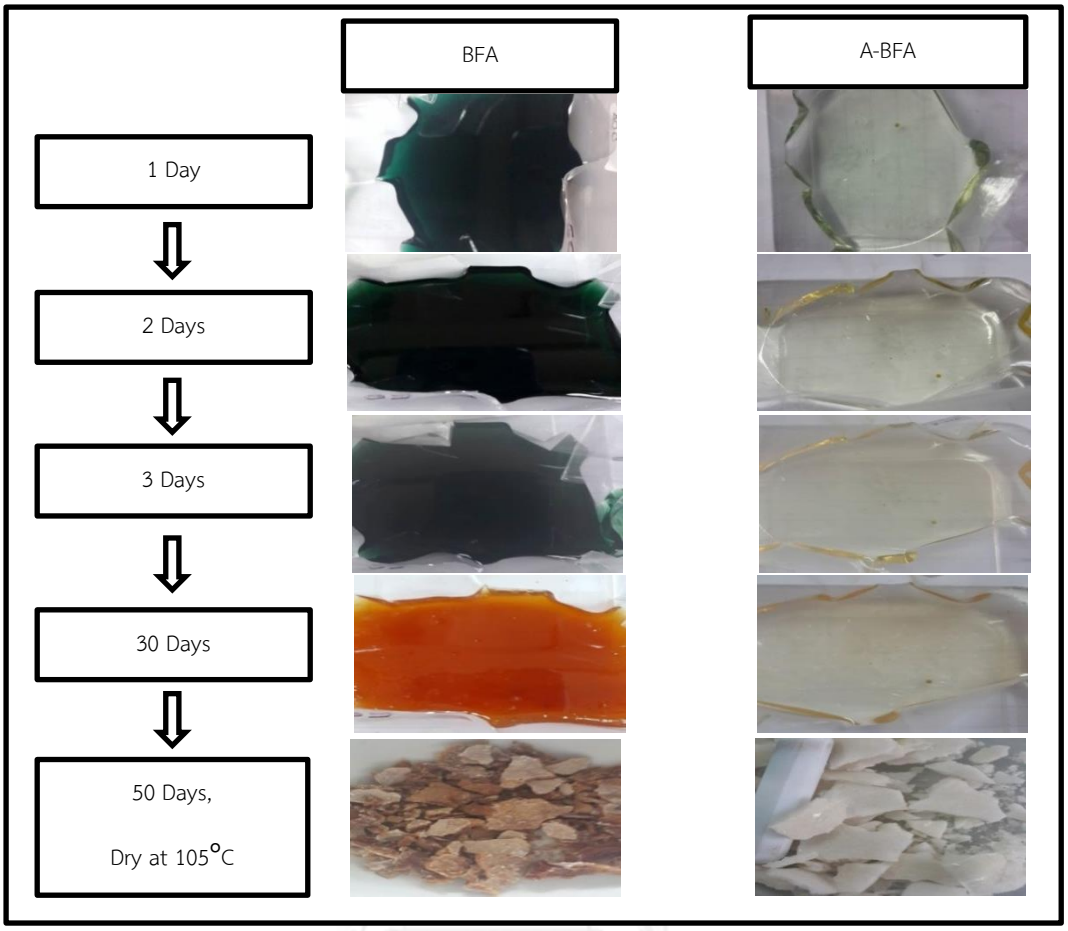

Figure 4.12 Polymerization of sodium silicate soluble

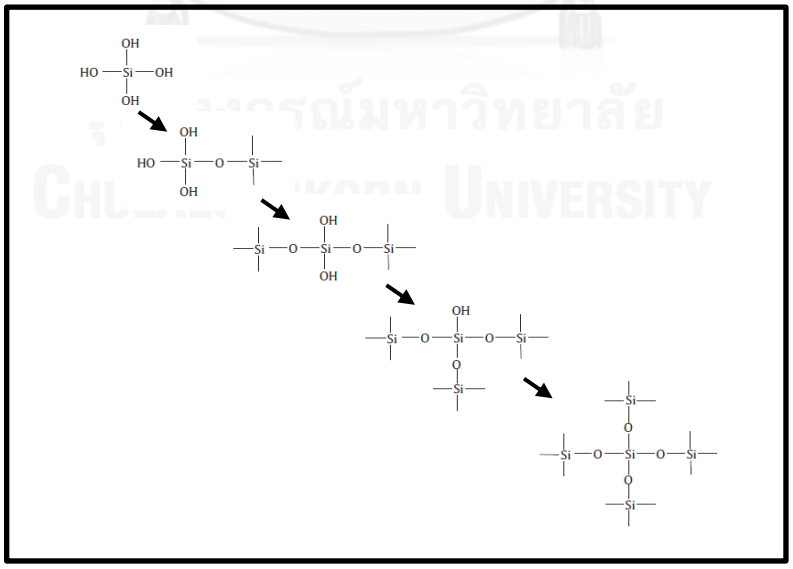

Figure 4.13 Polymerization pathway of pure silica

CHAPTER 5
CONCLUSIONS

5.1 Sodium silicate production

The production of sodium silicate from bagasse fly ash (BFA) and acid-bagasse fly ash (A-BFA) were subject to several parameters including: SiO_2:Na_2CO_3 mole ratio, fused temperature and reaction time. The reaction taken place was the fused reaction at high temperature between carbonate and silica whereby most organic carbons in the raw material were decomposed.

Major product from the fused reaction was sodium silicate which could mostly be dissolved in water and the remaining Na_2CO_3 was impurity in supernatant solution. The solid precipitation after dissolved contained some quartz-SiO_2, metal oxide and insoluble sodium silicate. Overall, the optimal condition of sodium silicate synthesis was 1:1.25 of SiO_2:Na_2CO_3 mole ratio at fused temperature of 830°C and reaction time of 60 minutes. Yield of soluble sodium silicate /insoluble sodium silicate was 38%/18% and 45%/18% for BFA and A-BFA, respectively.

Based on 1,000 grams of original BFA, soluble sodium silicate yield in supernatant/insoluble sodium silicate was 754/410 grams for the case without acid pretreatment and 892/365 grams for the case with acid pretreatment. Table 5.1 provides some important characteristics of sodium silicate production from the two raw materials.

Table 5.1 Mass distribution in solid product at optimal condition of sodium silicate synthesis (1,000 grams of original bagasse fly ash and 1,380 grams of Na_2CO_3)

Mass distribution in solid product		Silica source	
		BFA	A-BFA
Remaining raw materials (grams)	SiO_2	22	12
	Na_2CO_3	319	270
	Other	192	41
Products (grams)	Na_2SiO_3 (insoluble)	410	365
	Na_2SiO_3 (soluble)	**754**	**892**

5.2 Contribution and Recommendations

This work presents one potential usage of bagasse fly ash which is to convert it into sodium silicate. Typical practice in Thailand for bagasse fly ash is to land fill which does not only require land but also could lead to environmental issues such as leachate and greenhouse gas emission. The conversion of fly ash to useful chemical is in fact not new, and there are reports regarding such utilization such as the conversion of fly ash to zeolite or to silica sources. The method proposed in this work is simple and easy to upscale and can be further investigated to be a viable technology as there is a demand of sodium silicate for glass industry (coating agent), steel industry, detergent making, etc.

Certain issues need to be discussed further, and these are summarized as follows:

- The sodium silicate reaction was investigated molecules of intermediate such as $Na_2Si_2O_5$ (at 1:1.25 of SiO_2:Na_2CO_3 mole ratio, 830^{o}C) that showed at 30 min of reaction time. So, short reaction might be obtained other molecules of intermediates for completely sodium silicate synthesis.

- From the finding in this work, it can be concluded that the extent of reaction of silica to sodium silicate was controlled significantly by the extent of reaction. The silicate structure framework as silica in the raw material was changed to sodium silicates in two major forms, sheet silicates ($Si_2O_5^{2-}$) at low reaction extent, and single chain silicate (SiO_3^{2-}) at high reaction extent. High reaction extent occurred at relatively high temperature (greater than 830^{o}C) and high reaction time (greater than 60 min).

จุฬาลงกรณ์มหาวิทยาลัย
Chulalongkorn University

REFERENCES

Batra, V. S., S. Urbonaite and G. Svensson, 2008: Characterization of unburned carbon in bagasse fly ash. *Fuel,* **87,** 2972-2976.

Belviso, C., F. Cavalcante, F. Javier Huertas, A. Lettino, P. Ragone and S. Fiore, 2012: The crystallisation of zeolite (X-and A-type) from fly ash at 25 C in artificial sea water. *Microporous and Mesoporous Materials,* **162,** 115-121.

Belviso, C., F. Cavalcante, A. Lettino and S. Fiore, 2011: Effects of ultrasonic treatment on zeolite synthesized from coal fly ash. *Ultrasonics sonochemistry,* **18,** 661-668.

Blissett, R. and N. Rowson, 2012: A review of the multi-component utilisation of coal fly ash. *Fuel,* **97,** 1-23.

Bo, W. and M. Hongzhu, 1998: Factors affecting the synthesis of microsized NaY zeolite. *Microporous and mesoporous materials,* **25,** 131-136.

Böschel, D., M. Janich and H. Roggendorf, 2003: Size distribution of colloidal silica in sodium silicate solutions investigated by dynamic light scattering and viscosity measurements. *Journal of colloid and interface science,* **267,** 360-368.

Chareonpanich, M., T. Namto, P. Kongkachuichay and J. Limtrakul, 2004: Synthesis of ZSM-5 zeolite from lignite fly ash and rice husk ash. *Fuel processing technology,* **85,** 1623-1634.

Chindaprasirt, P. and K. Pimraksa, 2008: A study of fly ash–lime granule unfired brick. *Powder technology,* **182,** 33-41.

Cruz, D., S. Bulbulian, E. Lima and H. Pfeiffer, 2006: Kinetic analysis of the thermal stability of lithium silicates (Li< sub> 4</sub> SiO< sub> 4</sub> and Li< sub> 2</sub> SiO< sub> 3</sub>). *Journal of Solid State Chemistry,* **179,** 909-916.

Cultrone, G. and E. Sebastián, 2009: Fly ash addition in clayey materials to improve the quality of solid bricks. *Construction and Building Materials,* **23,** 1178-1184.

Davidovits, J., 2008: *Geopolymer chemistry and applications*. Geopolymer Institute.

Ding, Y., G. Yin, X. Liao, Z. Huang, X. Chen and Y. Yao, 2012: Key role of sodium silicate modulus in synthesis of mesoporous silica SBA-15 rods with controllable lengths and diameters. *Materials Letters,* **75,** 45-47.

Dong, D., J. Sun, F. Huang, Q. Gao, Y. Wang and R. Li, 2009: Using trifluoroacetic acid to pretreat lignocellulosic biomass. *Biomass and bioenergy,* **33,** 1719-1723.

Fernández-Pereira, C., J. De la Casa, A. Gómez-Barea, F. Arroyo, C. Leiva and Y. Luna, 2011: Application of biomass gasification fly ash for brick manufacturing. *Fuel,* **90,** 220-232.

Gaggiano, R., P. Moriamé, M. Biesemans, I. De Graeve and H. Terryn, 2011: Influence of SiO< sub> 2</sub>/Na< sub> 2</sub> O ratio and temperature on the mechanism of interaction of soluble sodium silicates with porous anodic alumina. *Surface and Coatings Technology,* **206,** 1269-1276.

Garbacz, A. and J. J. Sokołowska, 2013: Concrete-like polymer composites with fly ashes–Comparative study. *Construction and Building Materials,* **38,** 689-699.

Ge, Q., J. Shao, Z. Wang and Y. Yan, 2012: Effects of the synthesis hydrogel on the formation of zeolite LTA membranes. *Microporous and Mesoporous Materials,* **151,** 303-310.

Guo, F., Z.-G. Peng, J.-Y. Dai and Z.-L. Xiu, 2010: Calcined sodium silicate as solid base catalyst for biodiesel production. *Fuel Processing Technology,* **91,** 322-328.

Halina, M., S. Ramesh, M. Yarmo and R. Kamarudin, 2007: Non-hydrothermal synthesis of mesoporous materials using sodium silicate from coal fly ash. *Materials chemistry and physics,* **101,** 344-351.

Hovis, G. L., M. J. Toplis and P. Richet, 2004: Thermodynamic mixing properties of sodium silicate liquids and implications for liquid–liquid immiscibility. *Chemical geology,* **213,** 173-186.

Iyer, R., 2002: The surface chemistry of leaching coal fly ash. *Journal of hazardous materials,* **93,** 321-329.

Jorapur, R. and A. K. Rajvanshi, 1997: Sugarcane leaf-bagasse gasifiers for industrial heating applications. *Biomass and Bioenergy,* **13,** 141-146.

Karami, D. and S. Rohani, 2009: Synthesis of pure zeolite Y using soluble silicate, a two-level factorial experimental design. *Chemical Engineering and Processing: Process Intensification,* **48,** 1288-1292.

Karlfeldt Fedje, K., C. Ekberg, G. Skarnemark and B.-M. Steenari, 2010: Removal of hazardous metals from MSW fly ash—an evaluation of ash leaching methods. *Journal of hazardous materials,* **173,** 310-317.

Kashiwakura, S., H. Kubo, Y. Kumagai, H. Kubo, K. Matsubae-Yokoyama, K. Nakajima and T. Nagasaka, 2009: Removal of boron from coal fly ash by washing with HCl solution. *Fuel,* **88,** 1245-1250.

Kashiwakura, S., H. Ohno, K. Matsubae-Yokoyama, Y. Kumagai, H. Kubo and T. Nagasaka, 2010: Removal of arsenic in coal fly ash by acid washing process

using dilute H< sub> 2</sub> SO< sub> 4</sub> solvent. *Journal of hazardous materials,* **181,** 419-425.

Kim, Y. K., K. P. Rajesh and J.-S. Yu, 2013: Zeolite materials prepared using silicate waste from template synthesis of ordered mesoporous carbon. *Journal of hazardous materials,* **260,** 350-357.

Kow, K.-W., R. Yusoff, A. Aziz and E. Abdullah, 2014: From bamboo leaf to aerogel: Preparation of water glass as a precursor. *Journal of Non-Crystalline Solids,* **386,** 76-84.

Long, Y.-D., F. Guo, Z. Fang, X.-F. Tian, L.-Q. Jiang and F. Zhang, 2011: Production of biodiesel and lactic acid from rapeseed oil using sodium silicate as catalyst. *Bioresource technology,* **102,** 6884-6886.

Lucas, S., M. T. Tognonvi, J. Gelet, J. Soro and S. Rossignol, 2011: Interactions between silica sand and sodium silicate solution during consolidation process. *Journal of Non-Crystalline Solids,* **357,** 1310-1318.

Misran, H., R. Singh, S. Begum and M. A. Yarmo, 2007: Processing of mesoporous silica materials (MCM-41) from coal fly ash. *Journal of materials processing technology,* **186,** 8-13.

Musyoka, N. M., L. F. Petrik, E. Hums, H. Baser and W. Schwieger, 2012: In situ ultrasonic monitoring of zeolite A crystallization from coal fly ash. *Catalysis Today,* **190,** 38-46.

Oliveira, A., P. Malafaya and R. Reis, 2003: Sodium silicate gel as a precursor for the in vitro nucleation and growth of a bone-like apatite coating in compact and porous polymeric structures. *Biomaterials,* **24,** 2575-2584.

Panitchakarn, P., N. Laosiripojana, N. Viriya-umpikul and P. Pavasant, 2013: Synthesis of High Purity of NaA and NaX Zeolite from Coal Fly Ash. *Journal of the Air & Waste Management Association*.

Purnomo, C. W., C. Salim and H. Hinode, 2012: Synthesis of pure Na–X and Na–A zeolite from bagasse fly ash. *Microporous and Mesoporous Materials,* **162,** 6-13.

Ravikumar, D. and N. Neithalath, 2012: Reaction kinetics in sodium silicate powder and liquid activated slag binders evaluated using isothermal calorimetry. *Thermochimica Acta,* **546,** 32-43.

Round, C. I., S. J. Hill, K. Latham and C. D. Williams, 1997: The crystal morphology of zeolite A. The effects of the source of the reagents. *Microporous materials,* **11,** 213-225.

Ruangtaweep, Y., J. Kaewkhao, C. Kedkaew and P. Limsuwan, 2011: Investigation of biomass fly ash in Thailand for recycle to glass production. *Procedia Engineering,* **8,** 58-61.

TAN, H. and S.-r. WANG, 2009: Experimental study of the effect of acid-washing pretreatment on biomass pyrolysis. *Journal of Fuel Chemistry and Technology,* **37,** 668-672.

Umamaheswaran, K. and V. S. Batra, 2008: Physico-chemical characterisation of Indian biomass ashes. *Fuel,* **87,** 628-638.

Yamashita, S., H. Behrens, B. C. Schmidt and R. Dupree, 2008: Water speciation in sodium silicate glasses based on NIR and NMR spectroscopy. *Chemical Geology,* **256,** 231-241.

Yang, X., P. Roonasi and A. Holmgren, 2008: A study of sodium silicate in aqueous solution and sorbed by synthetic magnetite using in situ ATR-FTIR spectroscopy. *Journal of colloid and interface science,* **328,** 41-47.

Yilmaz, A. and N. Degirmenci, 2009: Possibility of using waste tire rubber and fly ash with Portland cement as construction materials. *Waste Management,* **29,** 1541-1546.

Yin, D. T., Q. Jing, W. W. AlDajani, S. Duncan, U. Tschirner, J. Schilling and R. J. Kazlauskas, 2011: Improved pretreatment of lignocellulosic biomass using enzymatically-generated peracetic acid. *Bioresource technology,* **102,** 5183-5192.

Yuan, M.-r., J.-t. Lu, G. Kong and C.-s. Che, 2011: Effect of silicate anion distribution in sodium silicate solution on silicate conversion coatings of hot-dip galvanized steels. *Surface and Coatings Technology,* **205,** 4466-4470.

Zhang, Z., I. M. O'Hara and W. O. Doherty, 2012: Pretreatment of sugarcane bagasse by acid-catalysed process in aqueous ionic liquid solutions. *Bioresource technology,* **120,** 149-156.

Zhao, Q., M. Guerette, G. Scannell and L. Huang, 2012: < i> In-situ</i> high temperature Raman and Brillouin light scattering studies of sodium silicate glasses. *Journal of Non-Crystalline Solids,* **358,** 3418-3426.

APPENDIX

จุฬาลงกรณ์มหาวิทยาลัย
Chulalongkorn University

Figure A.1 Raman spectra of sodium silicate soluble

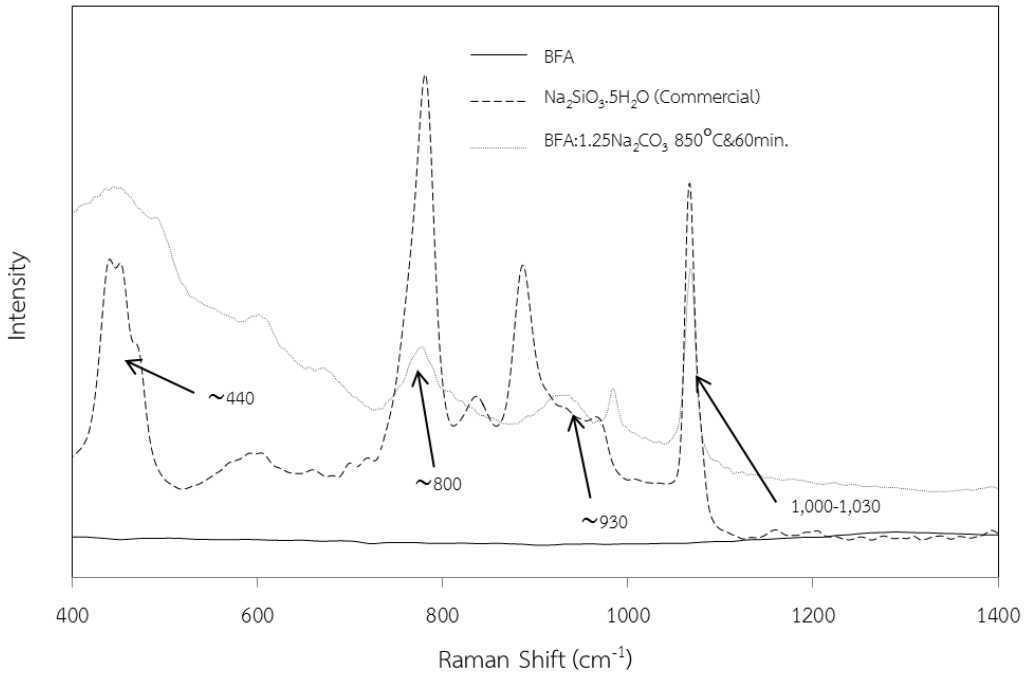

จุฬาลงกรณ์มหาวิทยาลัย
Chulalongkorn University

Figure A.2 Solid product at maximum yield of sodium silicate from BFA source

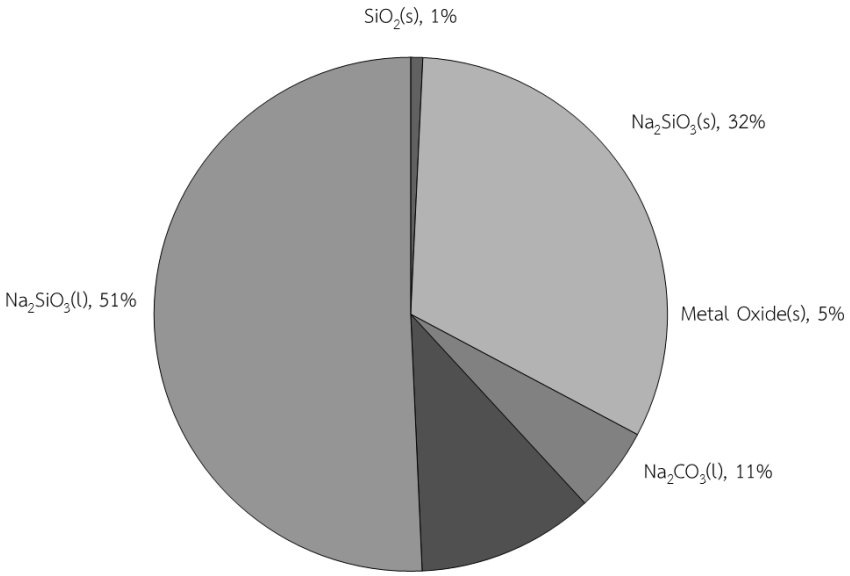

Figure A.3 Solid product at maximum yield of sodium silicate from A-BFA source

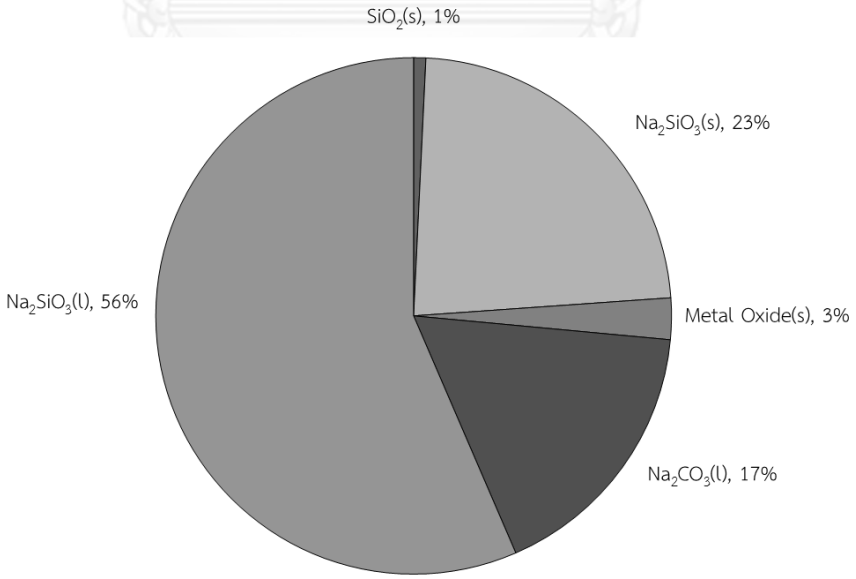

Table B.1 Mass distribution of solid products (%wt) from BFA source (650°C of fused temperature and 30 minutes of reaction time)

SiO_2:Na_2SO_3 mole ratio	Remaining Raw Materials			Product Na_2SiO_3	
	SiO_2	Na_2CO_3	Other	Soluble	Insoluble
1:0.00	75	0	25	0	0
1:0.50	34	20	15	0.6	26.4
1:0.75	24	25	13	1	31
1:1.00	21	38	11	1	24
1:1.25	19	48	9	1	18
1:1.50	16	52	8	1	18
1:1.75	16	58	7	1	14
1:2.00	15	64	7	1	9
1:2.25	14	68	6	1	7

Table B.2 Mass distribution of solid products (%wt) from A-BFA source (650°C of fused temperature and 30 minutes of reaction time)

SiO_2:Na_2SO_3 mole ratio	Remaining Raw Materials			Product Na_2SiO_3	
	SiO_2	Na_2CO_3	Other	Soluble	Insoluble
1:0.00	92	0	8	0	0
1:0.50	58	39	4	4	3
1:0.75	45	44	3	5	7
1:1.00	39	54	3	4	3
1:1.25	32	57	3	4	6
1:1.50	28	61	2	4	6
1:1.75	23	62	2	4	8
1:2.00	18	60	2	4	12
1:2.25	16	64	2	4	12

จุฬาลงกรณ์มหาวิทยาลัย
Chulalongkorn University

Table B.3 Mass distribution of solid products (%wt) from BFA source (750°C of fused temperature and 30 minutes of reaction time)

SiO_2:Na_2SO_3 mole ratio	Remaining Raw Materials			Product Na_2SiO_3	
	SiO_2	Na_2CO_3	Other	Soluble	Insoluble
1:0.00	75	0	25	0	0
1:0.50	30	14	15	2	29
1:0.75	23	24	12	2	30
1:1.00	18	33	10	2	26
1:1.25	15	39	9	3	24
1:1.50	13	45	8	3	22
1:1.75	13	53	8	2	17
1:2.00	11	57	7	2	15
1:2.25	9	58	6	2	18

Table B.4 Mass distribution of solid products (%wt) from A-BFA source (750°C of fused temperature and 30 minutes of reaction time)

SiO_2:Na_2SO_3 mole ratio	Remaining Raw Materials			Product Na_2SiO_3	
	SiO_2	Na_2CO_3	Other	Soluble	Insoluble
1:0.00	92	0	8	0	0
1:0.50	46	14	4	7	30
1:0.75	38	34	3	7	15
1:1.00	33	46	3	6	11
1:1.25	27	49	3	6	14
1:1.50	22	52	2	6	15
1:1.75	18	53	2	6	18
1:2.00	18	60	2	6	12
1:2.25	11	54	2	5	18

จุฬาลงกรณ์มหาวิทยาลัย
Chulalongkorn University

Table B.5 Mass distribution of solid products (%wt) from BFA source (800°C of fused temperature and 30 minutes of reaction time)

SiO_2:Na_2SO_3 mole ratio	Remaining Raw Materials			Product Na_2SiO_3	
	SiO_2	Na_2CO_3	Other	Soluble	Insoluble
1:0.00	75	0	25	0	0
1:0.50	22	0	15	12	35
1:0.75	13	7	12	11	41
1:1.00	10	20	10	24	28
1:1.25	8	27	9	15	27
1:1.50	6	33	8	14	24
1:1.75	6	42	7	11	20
1:2.00	4	42	6	10	21
1:2.25	3	47	6	11	20

Table B.6 Mass distribution of solid products (%wt) from A-BFA source (800°C of fused temperature and 30 minutes of reaction time)

SiO_2:Na_2SO_3 mole ratio	Remaining Raw Materials			Product Na_2SiO_3	
	SiO_2	Na_2CO_3	Other	Soluble	Insoluble
1:0.00	92.	0	8	0	0
1:0.50	37	0	4	15	37
1:0.75	31	21	4	23	15
1:1.00	28	36	3	15	14
1:1.25	26	48	3	14	6
1:1.50	22	52	2	13	8
1:1.75	20	56	2	10	9
1:2.00	16	58	2	10	9
1:2.25	16	64	2	9	6

จุฬาลงกรณ์มหาวิทยาลัย
Chulalongkorn University

Table B.7 Mass distribution of solid products (%wt) from BFA source (830°C of fused temperature and 30 minutes of reaction time)

SiO_2:Na_2SO_3 mole ratio	Remaining Raw Materials			Product Na_2SiO_3	
	SiO_2	Na_2CO_3	Other	Soluble	Soluble
1:0.00	75	0	25	0	0
1:0.50	0	0	0	0	0
1:0.75	9	0	12	18	39
1:1.00	5	10	10	22	32
1:1.25	2	15	10	21	34
1:1.50	22	26	8	18	29
1:1.75	1	32	7	15	27
1:2.00	1	38	6	14	22
1:2.25	1	42	6	12	20

Table B.8 Mass distribution of solid products (%wt) from A-BFA source (830°C of fused temperature and 30 minutes of reaction time)

SiO_2:Na_2SO_3 mole ratio	Remaining Raw Materials			Product Na_2SiO_3	
	SiO_2	Na_2CO_3	Other	Soluble	Insoluble
1:0.00	92	0	8	0	0
1:0.50	0	0	0	0	0
1:0.75	18	0	3	26	37
1:1.00	5	0	3	35	37
1:1.25	5	20	2	33	32
1:1.50	4	19	2	30	28
1:1.75	3	27	2	29	24
1:2.00	4	37	2	18	23
1:2.25	6	44	1	16	19

จุฬาลงกรณ์มหาวิทยาลัย
Chulalongkorn University

Table B.9 Mass distribution of solid products (%wt) from BFA source (850°C of fused temperature and 30 minutes of reaction time)

SiO_2:Na_2SO_3 mole ratio	Remaining Raw Materials			Product Na_2SiO_3	
	SiO_2	Na_2CO_3	Other	Soluble	Insoluble
1:0.00	75	0	25	0	0
1:0.50	0	0	0	0	0
1:0.75	9	0	12	16	41
1:1.00	4	7	10	24	31
1:1.25	2	16	8	22	27
1:1.50	1	22	7	17	27
1:1.75	1	29	6	14	22
1:2.00	1	33	5	14	20
1:2.25	1	39	5	12	18

Table B.10 Mass distribution of solid products (%wt) from A-BFA source (850°C of fused temperature and 30 minutes of reaction time)

SiO_2:Na_2SO_3 mole ratio	Remaining Raw Materials			Product Na_2SiO_3	
	SiO_2	Na_2CO_3	Other	Soluble	Insoluble
1:0.00	92	0	8	0	0
1:0.50	0	0	0	0	0
1:0.75	0	0	0	0	0
1:1.00	9	3	3	27	38
1:1.25	2	4	2	43	26
1:1.50	0	9	2	45	23
1:1.75	0	13	1	40	21
1:2.00	0	17	1	37	20
1:2.25	0	23	1	35	19

จุฬาลงกรณ์มหาวิทยาลัย
Chulalongkorn University

Table B.11 Mass distribution of solid products (%wt) from BFA source (650°C of fused temperature and 60 minutes of reaction time)

SiO_2:Na_2SO_3 mole ratio	Remaining Raw Materials			Product Na_2SiO_3	
	SiO_2	Na_2CO_3	Other	Soluble	Insoluble
1:0.00	75	0	25	0	0
1:0.50	34	19	15	2	24
1:0.75	27	31	12	2	22
1:1.00	22	38	10	2	21
1:1.25	18	46	9	2	19
1:1.50	15	49	9	1	21
1:1.75	13	54	7	2	18
1:2.00	12	58	6	2	15
1:2.25	10	60	6	2	15

Table B.12 Mass distribution of solid products (%wt) from A-BFA source (650°C of fused temperature and 60 minutes of reaction time)

SiO_2:Na_2SO_3 mole ratio	Remaining Raw Materials			Product Na_2SiO_3	
	SiO_2	Na_2CO_3	Other	Soluble	Insoluble
1:0.00	92	0	8	0	0
1:0.50	53	24	4	4	24
1:0.75	41	36	4	3	23
1:1.00	34	46	3	3	20
1:1.25	28	50	3	3	19
1:1.50	24	56	2	3	17
1:1.75	20	59	2	3	17
1:2.00	18	63	2	2	15
1:2.25	17	67	2	2	14

จุฬาลงกรณ์มหาวิทยาลัย
Chulalongkorn University

Table B.13 Mass distribution of solid products (%wt) from BFA source (750°C of fused temperature and 60 minutes of reaction time)

SiO_2:Na_2SO_3 mole ratio	Remaining Raw Materials			Product Na_2SiO_3	
	SiO_2	Na_2CO_3	Other	Soluble	Insoluble
1:0.00	75	0	25	0	0
1:0.50	31	15	14	3	26
1:0.75	24	26	12	4	24
1:1.00	22	40	10	4	12
1:1.25	18	45	9	5	12
1:1.50	15	49	8	6	13
1:1.75	14	54	7	3	12
1:2.00	12	58	6	3	12
1:2.25	11	60	6	3	11

Table B.14 Mass distribution of solid products (%wt) from A-BFA source (750°C of fused temperature and 60 minutes of reaction time)

SiO_2:Na_2SO_3 mole ratio	Remaining Raw Materials			Product Na_2SiO_3	
	SiO_2	Na_2CO_3	Other	Soluble	Insoluble
1:0.00	92	0	8	0	0
1:0.50	50	25	4	7	15
1:0.75	39	34	4	7	17
1:1.00	34	47	3	10	7
1:1.25	28	50	3	9	11
1:1.50	24	55	3	8	10
1:1.75	22	61	2	7	7
1:2.00	20	65	1	7	5
1:2.25	15	64	1	6	12

จุฬาลงกรณ์มหาวิทยาลัย
Chulalongkorn University

Table B.15 Mass distribution of solid products (%wt) from BFA source (800°C of fused temperature and 60 minutes of reaction time)

SiO_2:Na_2SO_3 mole ratio	Remaining Raw Materials			Product Na_2SiO_3	
	SiO_2	Na_2CO_3	Other	Soluble	Insoluble
1:0.00	75	0	25	0	0
1:0.50	20	0	14	14	37
1:0.75	13	6	13	23	31
1:1.00	10	19	10	27	19
1:1.25	5	22	10	23	27
1:1.50	0	23	9	27	27
1:1.75	5	41	8	16	20
1:2.00	5	47	7	14	6
1:2.25	4	50	6	14	17

Table B.16 Mass distribution of solid products (%wt) from A-BFA source (800°C of fused temperature and 60 minutes of reaction time)

SiO_2:Na_2SO_3 mole ratio	Remaining Raw Materials			Product Na_2SiO_3	
	SiO_2	Na_2CO_3	Other	Soluble	Insoluble
1:0.00	92	0	8	0	0
1:0.50	39	1	4	16	37
1:0.75	28	24	4	14	36
1:1.00	27	34	3	10	21
1:1.25	24	43	2	11	16
1:1.50	18	46	2	10	21
1:1.75	12	42	2	8	23
1:2.00	12	52	2	9	20
1:2.25	10	55	1	9	19

จุฬาลงกรณ์มหาวิทยาลัย
Chulalongkorn University

Table B.17 Mass distribution of solid products (%wt) from BFA source (830°C of fused temperature and 60 minutes of reaction time)

SiO_2:Na_2SO_3 mole ratio	Remaining Raw Materials			Product Na_2SiO_3	
	SiO_2	Na_2CO_3	Other	Soluble	Insoluble
1:0.00	75	0	25	0	0
1:0.50	0	0	0	0	0
1:0.75	6	0	12	27	33
1:1.00	1	3	10	35	27
1:1.25	1	15	9	35	19
1:1.50	0.5	23	8	29	18
1:1.75	0.5	33	7	34	13
1:2.00	0.5	40	7	29	13
1:2.25	0.5	44	6	25	13

Table B.18 Mass distribution of solid products (%wt) from A-BFA source (830°C of fused temperature and 60 minutes of reaction time)

SiO_2:Na_2SO_3 mole ratio	Remaining Raw Materials			Product Na_2SiO_3	
	SiO_2	Na_2CO_3	Other	Soluble	Insoluble
1:0.00	92	0	8	0	0
1:0.50	0	0	0	0	0
1:0.75	17	0	4	22	45
1:1.00	8	0	3	43	29
1:1.25	1	0	3	55	22
1:1.50	0.5	14	2	47	19
1:1.75	0.5	25	2	50	14
1:2.00	0.5	32	2	43	13
1:2.25	0.3	38	2	38	13

จุฬาลงกรณ์มหาวิทยาลัย
Chulalongkorn University

Table B.19 Mass distribution of solid products (%wt) from BFA source (850°C of fused temperature and 60 minutes of reaction time)

SiO_2:Na_2SO_3 mole ratio	Remaining Raw Materials			Product Na_2SiO_3	
	SiO_2	Na_2CO_3	Other	Soluble	Insoluble
1:0.00	75	0	25	0	0
1:0.50	0	0	0	0	0
1:0.75	10	0	12	24	34
1:1.00	4	7	10	32	33
1:1.25	1	14	8	32	20
1:1.50	1	23	8	27	18
1:1.75	1	29	7	23	17
1:2.00	0	0	0	0	0
1:2.25	0	0	0	0	0

Table B.20 Mass distribution of solid products (%wt) from A-BFA source (850°C of fused temperature and 60 minutes of reaction time)

SiO_2:Na_2SO_3 mole ratio	Remaining Raw Materials			Product Na_2SiO_3	
	SiO_2	Na_2CO_3	Other	Soluble	Insoluble
1:0.00	92	0	8	0	0
1:0.50	0	0	0	0	0
1:0.75	0	0	0	0	0
1:1.00	0	0	0	0	0
1:1.25	0	6	2	52	18
1:1.50	0	15	2	46	16
1:1.75	0	22	2	42	14
1:2.00	0	23	1	44	14
1:2.25	0	31	1	38	13

จุฬาลงกรณ์มหาวิทยาลัย
Chulalongkorn University

Table B.21 Mass distribution of solid products (%wt) from BFA source (650°C of fused temperature and 120 minutes of reaction time)

SiO_2:Na_2SO_3 mole ratio	Remaining Raw Materials			Product Na_2SiO_3	
	SiO_2	Na_2CO_3	Other	Soluble	Insoluble
1:0.00	75	0	25	0	0
1:0.50	40	31	14	4	6
1:0.75	31	38	12	4	9
1:1.00	26	47	10	4	7
1:1.25	22	51	9	4	8
1:1.50	22	60	8	3	2
1:1.75	17	61	7	4	5
1:2.00	15	64	6	4	4
1:2.25	15	67	6	4	3

Table B.22 Mass distribution of solid products (%wt) from A-BFA source (650°C of fused temperature and 120 minutes of reaction time)

SiO_2:Na_2SO_3 mole ratio	Remaining Raw Materials			Product Na_2SiO_3	
	SiO_2	Na_2CO_3	Other	Soluble	Insoluble
1:0.00	92	0	8	0	0
1:0.50	54	33	4	6	5
1:0.75	42	41	3	6	7
1:1.00	34	45	3	6	12
1:1.25	31	56	2	6	3
1:1.50	20	47	2	5	13
1:1.75	20	58	2	6	11
1:2.00	16	58	2	6	14
1:2.25	15	63	2	6	122

จุฬาลงกรณ์มหาวิทยาลัย
Chulalongkorn University

Table B.23 Mass distribution of solid products (%wt) from BFA source (750°C of fused temperature and 120 minutes of reaction time)

SiO_2:Na_2SO_3 mole ratio	Remaining Raw Materials			Product Na_2SiO_3	
	SiO_2	Na_2CO_3	Other	Soluble	Insoluble
1:0.00	75	0	25	0	0
1:0.50	32	19	14	6	17
1:0.75	24	26	12	7	19
1:1.00	21	38	10	7	11
1:1.25	17	43	8	9	10
1:1.50	13	45	8	12	10
1:1.75	15	56	7	7	6
1:2.00	13	59	6	6	6
1:2.25	11	60	6	6	8

Table B.24 Mass distribution of solid products (%wt) from A-BFA source (750°C of fused temperature and 120 minutes of reaction time)

SiO_2:Na_2SO_3 mole ratio	Remaining Raw Materials			Product Na_2SiO_3	
	SiO_2	Na_2CO_3	Other	Soluble	Insoluble
1:0.00	92	0	8	0	0
1:0.50	45	12	4	12	25
1:0.75	33	24	4	10	25
1:1.00	28	36	3	9	21
1:1.25	23	41	3	9	21
1:1.50	21	50	2	9	15
1:1.75	18	55	2	9	13
1:2.00	15	56	2	9	17
1:2.25	14	61	2	8	14

จุฬาลงกรณ์มหาวิทยาลัย
Chulalongkorn University

Table B.25 Mass distribution of solid products (%wt) from BFA source (800°C of fused temperature and 120 minutes of reaction time)

SiO_2:Na_2SO_3 mole ratio	Remaining Raw Materials			Product Na_2SiO_3	
	SiO_2	Na_2CO_3	Other	Soluble	Insoluble
1:0.00	75	0	25	0	0
1:0.50	22	0	14	0	45
1:0.75	7	0	12	20	41
1:1.00	12	22	10	14	24
1:1.25	9	29	9	13	23
1:1.50	7	34	8	13	22
1:1.75	6	39	7	13	18
1:2.00	3	40	6	12	20
1:2.25	2	44	6	12	20

Table B.26 Mass distribution of solid products (%wt) from A-BFA source (800°C of fused temperature and 120 minutes of reaction time)

SiO_2:Na_2SO_3 mole ratio	Remaining Raw Materials			Product Na_2SiO_3	
	SiO_2	Na_2CO_3	Other	Soluble	Insoluble
1:0.00	92	0	8	0	0
1:0.50	39	5	4	10	35
1:0.75	23	7	3	25	27
1:1.00	15	12	3	23	33
1:1.25	12	23	3	24	26
1:1.50	14	37	2	13	23
1:1.75	13	45	2	14	20
1:2.00	9	45	2	13	22
1:2.25	9	51	2	13	20

จุฬาลงกรณ์มหาวิทยาลัย
Chulalongkorn University

Table B.27 Mass distribution of solid products (%wt) from BFA source (830°C of fused temperature and 120 minutes of reaction time)

SiO_2:Na_2SO_3 mole ratio	Remaining Raw Materials			Product Na_2SiO_3	
	SiO_2	Na_2CO_3	Other	Soluble	Insoluble
1:0.00	75	0	25	0	0
1:0.50	0	0	0	0	0
1:0.75	7	0	12	20	40
1:1.00	6	10	10	27	23
1:1.25	2	15	9	26	21
1:1.50	1	22	7	25	21
1:1.75	0.5	28	7	22	19
1:2.00	0.2	35	6	21	17
1:2.25	0.8	41	6	22	13

Table B.28 Mass distribution of solid products (%wt) from A-BFA source (830°C of fused temperature and 120 minutes of reaction time)

SiO_2:Na_2SO_3 mole ratio	Remaining Raw Materials			Product Na_2SiO_3	
	SiO_2	Na_2CO_3	Other	Soluble	Insoluble
1:0.00	92	0	8	0	0
1:0.50	0	0	0	0	0
1:0.75	0	0	0	0	0
1:1.00	21	24	3	25	12
1:1.25	3	7	3	51	18
1:1.50	0.3	13	2	50	15
1:1.75	0	19	2	42	19
1:2.00	0	24	2	40	22
1:2.25	0	33	2	32	19

จุฬาลงกรณ์มหาวิทยาลัย
Chulalongkorn University

Table B.29 Mass distribution of solid products (%wt) from BFA source (850°C of fused temperature and 120 minutes of reaction time)

SiO_2:Na_2SO_3 mole ratio	Remaining Raw Materials			Product Na_2SiO_3	
	SiO_2	Na_2CO_3	Other	Soluble	Insoluble
1:0.00	75	0	25	0	0
1:0.50	0	0	0	0	0
1:0.75	0	0	0	0	0
1:1.00	2	4	10	31	30
1:1.25	0	10	9	35	22
1:1.50	0	0	0	0	0
1:1.75	0	0	0	0	0
1:2.00	0	0	0	0	0
1:2.25	0	0	0	0	0

Table B.30 Mass distribution of solid products (%wt) from A-BFA source (850°C of fused temperature and 120 minutes of reaction time)

SiO_2:Na_2SO_3 mole ratio	Remaining Raw Materials			Product Na_2SiO_3	
	SiO_2	Na_2CO_3	Other	Soluble	Insoluble
1:0.00	92	0	8	0	0
1:0.50	0	0	0	0	0
1:0.75	0	0	0	0	0
1:1.00	0	8	2	31	28
1:1.25	0	2	2	43	32
1:1.50	0	8	2	46	23
1:1.75	0	21	2	35	22
1:2.00	0	27	2	32	20
1:2.25	0	0	0	0	0

จุฬาลงกรณ์มหาวิทยาลัย
Chulalongkorn University

VITA

Miss Titimat Suksawastsak was born on February 8th, 1989 in Surat thani, Thailand. She received a Bachelor's Degree of Chemical Engineering from the Faculty of Engineering and Industrial Technology, Silpakorn University in 2010. She continued her further study for a Master's Degree of Chemical Engineering at Chulalongkorn University. She participated in the Environmental Chemical Engineering and Safety Research Laboratory. She finally achieved her Master's Degree in 2013.

จุฬาลงกรณ์มหาวิทยาลัย
CHULALONGKORN UNIVERSITY

จุฬาลงกรณ์มหาวิทยาลัย
Chulalongkorn University